



Transilvania
University
of Brasov

INTERDISCIPLINARY DOCTORAL SCHOOL

Faculty of Mechanical Engineering

Eng. Mihaela-Andreea IFTIMICIUC

DOCTORAL THESIS

ABSTRACT / REZUMAT

Scientific supervisor

Prof. Dr. Eng. Simona LACHE

BRAŞOV, 2021

Eng. Mihaela – Andreea IFTIMICIUC

DOCTORAL THESIS

Mechanically Expanded Pyramidal Cellular Structures for Sandwich Panels

Structuri celulare piramidale expandate mecanic pentru panouri sandwich

Doctoral field: Mechanical Engineering

ABSTRACT / REZUMAT

To Mrs./ Mr.

Review Board of the Doctorat Thesis

Enforced by the Decision of the Rector of the Transilvania University of Brașov

No. 11321 / 21.07.2021

PRESIDENT: Prof. Dr. Eng. Ioan-Călin ROȘCA, Transilvania University of Brașov

SCIENTIFIC SUPERVISOR: Prof. Dr. Eng. Simona LACHE Transilvania University of Brașov

OFFICIAL REVIEWERS: Prof. Dr. Eng. Dirk VANDEPITTE, Katholieke Universiteit
Leuven

Prof. Dr. Eng. Anton HADĂR, University Politehnica of Bucharest

Prof. Dr. Eng. Sorin VLASE, Transilvania University of
Brașov

Date, time and place of the public defence of the doctoral thesis:

24th of September 2021, at 09.00, room UII3.

Any appreciations or comments on the content of the doctoral thesis will be sent in time, by email, to the following address: mihaela.iftimiciuc@unitbv.ro.

At the same time, you are kindly invited to take part in the public session of the thesis' defense.

Thank you.

CONTENT

	Pg. Abstract	Pg. Thesis
Foreword	4	13
Acknowledgements	5	14
Introduction.....	6	15
1. Critical review of the state of the art on the construction of sandwich panels	8	17
1.1 General considerations	8	17
1.2 Types of cellular cores used for the construction of sandwich panels.....	9	19
1.2.1 Periodic cellular structures	9	19
■ Periodic cellular cores with open or closed topology.....	9	19
■ Lattice truss cellular cores	9	20
1.2.2 Stochastic cellular structures.....	10	21
1.2.3 Hierarchical cellular structures.....	10	21
1.3 Materials and technologies used in the construction of sandwich panels	11	22
1.3.1 Materials and technologies used for the fabrication of the face sheets	11	22
1.3.2 Materials and technologies used for the construction of cellular cores	12	25
■ Mechanical expansion	12	26
■ Cold forming	13	27
■ Thermal forming	13	28
■ Additive manufacturing	13	29
■ Weaving of metallic wires	13	30
■ Folding techniques	13	31
1.4 Critical analysis of the state of the art	14	32
1.5 Conclusions of the state-of-the-art review	15	36
2. Research goals and objectives	16	38
3. Study of the novel pyramidal cellular structure for the construction of sandwich panels	17	39
3.1 Novel pyramidal cellular structure and its manufacturing principle	17	39
3.2 Parametric study of the cellular topology	19	41
3.3 Trapezoidal cellular structure	22	48
3.4 Comparative study	26	55
3.5 Conclusions.....	28	59
4. Theoretical and experimental analysis of the novel pyramidal cellular structure	29	61
4.1 Out-of-plane compression properties of the unit cell	29	61
4.1.1 Analytical modelling.....	29	61
4.1.2 Numerical investigation of the buckling modes of the cellular structure.....	32	66

4.1.3	Experimental approach	32	68
■	Sample preparation.....	32	68
■	Investigated geometric configurations	32	69
4.2	Validation of the theoretical model.....	33	70
4.3	Trapezoidal cellular structure	35	78
4.4	The variation of the internal angle	37	82
4.5	Comparative study	38	84
4.6	Conclusions.....	39	86
5.	Theoretical and experimental analysis of the sandwich panel with metallic pyramidal core	40	87
5.1	Investigation of the bending stiffness.....	40	87
5.1.1	Numerical modelling	40	87
5.1.2	Analysis on the geometric imperfections.....	41	90
5.1.3	Experimental approach	42	92
■	Manufacturing of specimens	42	92
■	Investigation of geometric configurations	43	93
■	Experimental protocol	44	94
5.2	Validation of the numerical model - correlation between numerical and experimental results ..	45	95
5.3	Comparative study	48	105
5.4	Conclusions.....	49	108
6.	General conclusions and original contributions.....	51	109
References	55	113

Foreword

This doctoral thesis entitled *Mechanically Expanded Pyramidal Cellular Structures for Sandwich Panels* has been a challenging yet rewarding personal experience. I would like to express my highest gratitude, appreciation and respect to my scientific coordinator, Prof. Dr. Eng. Simona Lache, first of all, for believing in me. Her patience and academic rigor have constantly motivated me to overstep my boundaries and have shaped me into the scientist I am today. "*You will always be my professional role model*".

The periodic cellular structure on which this thesis is based was developed by Assoc. Prof. Dr. Eng. Marian N. Velea from Transilvania University of Brașov. He was the first to introduce me to the sandwich concept during my master's years and I am grateful for trusting me with his idea. I would like to thank him for his patience, kind words, constant encouragement and scientific expertise which brought a significant contribution to my professional development. I am humbled and appreciative for his every personal advice. "*I wouldn't have been here if it weren't for you*".

I would like to thank the other members of my scientific guiding committee, Prof. Dr. Eng. Călin Ioan Roșca and Prof. Dr. Eng. Sorin Vlase for their constructive remarks regarding my research work and to Lect. dr. Eng. Alexandru Cătălin Filip for his valuable help with the sample manufacturing process. His involvement has been most helpful for my experimental work.

During my PhD work I had the opportunity to conduct the experimental work through two doctoral research stages within two prestigious universities with seniority in this research field, KTH, Sweden and KU Leuven, Belgium. These opportunities have had a high influence on the quality of my research.

In this regard, I would like to thank Assoc. Prof. Dr. Eng Per Wennhage from the Lightweight Structures Laboratory at the Royal Institute of technology, KTH Sweden for his scientific expertise and support with both my experimental and theoretical work. The technical support of the Lightweight Structures group members at KTH is also acknowledged.

I would also like to express my sincere gratitude to Prof. Dr. Eng. Dirk Vandepitte for welcoming me into the Department of Mechanical Engineering at KU Leuven, Belgium to conduct a part of my experimental work. His scientific contributions and support have been most valuable for my professional development and have had a significant contribution in building up my confidence as a future scientist.

Last, but not least, I would like to express a heartfelt thank you to my parents for their steady support during the completion of my PhD and to my fiancé for his help, constant encouragement and emotional support throughout this entire process.

Acknowledgements

The research stages I have benefitted throughout my forming years were financially supported by Transilvania University of Brasov, throughout a special program dedicated to PhD students for short term research stages.

Introduction

The design and development of lightweight structures has emerged together with the building of the first aircrafts. The technology of the time has led to the design of the first lightweight structures based on low density natural materials, such as: wood, cork, natural foams etc.

Since the need to increase the comfort of everyday life has always been considered a challenge, the optimization of lightweight structures became a necessity to provide multi-functionality and ensure implementation in various industries and fields. Due to this, the extensive research in the field of advanced lightweight materials conducted up to the present offers a wide range of solutions.

Cellular structures, stochastic (foams) and periodic (honeycomb), have proven to be effective in reducing the weight of mechanical systems while providing high and stable structural performances.

Despite their high strength to weight ratio, these cellular structures are rarely used independently but are usually found in different assemblies. An example of a complex lightweight structure is the sandwich panel. These assemblies have been successfully used in the aerospace, naval, and automotive industries since their development and up to the present.

The construction of sandwich panels is constantly developing to keep up with the requirements of modern life. Nowadays, the numerous solutions present on the market provide complex assemblies with outstanding mechanical properties. High strength-to-weight ratios, considerable impact energy absorption capabilities and efficient control of acoustic noise and vibrations transfer, are only a few of the advantages provided by these mechanical structures.

Nonetheless, there are also a series of disadvantages worth mentioning when discussing the construction of sandwich panels. The high costs of the existing manufacturing technologies, the limited capability of generating complex geometries and the difficulty associated with the assembling of its components are only a few of the drawbacks of these types of structures.

The afore mentioned issues are subject of continuous research conducted on this topic to provide performant and versatile structures with multi-functional capacities. The main objective remains to design, develop, and optimize new structures obtained through simple and cost-efficient manufacturing technologies while reducing the carbon footprint as they go forward.

In this regard, the present research aims to study and provide a novel solution for the industry of sandwich construction, which can ensure a cost-efficient manufacturing method as well as a reduction of material loss within the process.

A brief overview of the research conducted throughout this doctoral thesis is presented below.

Chapter one presents a general overview on the development of lightweight mechanical structures, discussing the diversity of materials and technologies used in the construction of sandwich panels. This

is followed by a critical review of the state of the art which ends with the formulation of the research objectives established for the present thesis.

Chapter two is dedicated to presenting the research goals and objectives followed throughout the thesis.

In chapter three, a novel periodic cellular structure is proposed and investigated. The manufacturing method, based on mechanical expansion, is described in detail and the advantages provided are highlighted. A topologic study is performed in order define the relations for computing the gauge dimensions of the corrugation after the mechanical expansion process. A parametric study is later conducted, for understanding the influence of the manufacturing method on the geometrical parameters identified on the isolated unit cell of the corrugation.

Chapter four discusses the analytical model designed to compute the out-of-plane strength and stiffness of the pyramidal unit cell. The experimental model used to validate the theoretical formulation is also detailed and discussed. The chapter ends with a comparative study between the novel pyramidal core and other existing geometries, which is performed to assess the potential of the novel corrugation under study.

In chapter five, the bending and shear properties of the sandwich panel based on the pyramidal corrugation are investigated, by using both the numerical and experimental approach. A correlation between the two models is established. The last part of the chapter presents a comparative study between different solutions proposed in the literature and the advantages of the novel periodic cellular core are highlighted.

In chapter six the original contributions and general conclusions of the present doctoral thesis are formulated. In addition, suggestions for future studies are introduced and discussed.

1. Critical review of the state of the art on the construction of sandwich panels

1.1 General considerations

A sandwich panel is a complex mechanical structure containing three main components; two thin and rigid exterior faces placed on each side of a thick cellular core. The core is connected to the face sheets with the help of specific bonding methods (bonding using resin-based adhesives, welding, brazing etc.), Figure 1.1. The role of the adhesive layer is to determine the face sheets and core to act as a unitary structure and according to the norm it should sustain the same shear loads as the cellular core.

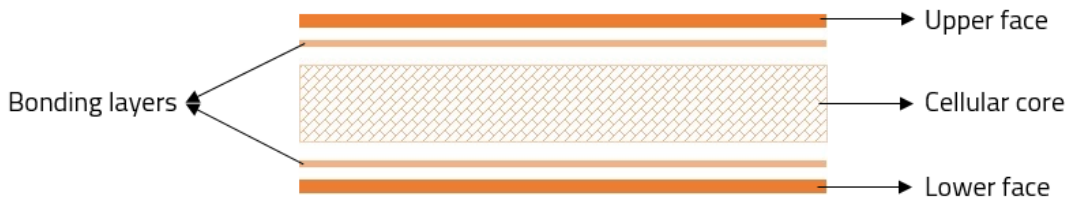


Figure 1.1 Transversal section through a sandwich panel.

The cellular core is required to maintain a constant distance between the face sheets and keep them stabilized to prevent local buckling effects. It also needs to allow the transfer of axial and transversal loads between the core and exterior faces.

The exterior faces sustain compressive and tensile loads and provide bending and in-plane shear stiffness to the entire assembly [1, 2, 3, 4, 5, 6].

The sandwich concept has become widely used when considering structural weight reduction and energy saving with the main advantage of providing a high strength-to-weight ratio as well as considerable impact energy absorption capabilities and efficient control of acoustic noise and vibrations transfer [7,8, 9, 10].

Nonetheless, when discussing the design and construction of sandwich panels, new challenges are rising together with their development: *i*) the high costs of the existent manufacturing technologies, *ii*) the limited capability of generating complex topologies and *iii*) the difficulty associated with the assembling of the components.

The main purpose of the extensive research in this field is represented by the necessity of developing new cellular topologies with high structural performances together with simple manufacturing technologies, to reduce the production costs and material loss during fabrication [2].

The real utility of implementing the use of lightweight structure in a multitude of industries can be motivated by a thorough examination of the effects pollution has on the environment.

A practical example is represented by the automotive industry where the release of toxic emissions into the atmosphere was regulated since 1992 together with adopting the EU1 standard by the European Council. This standard contains the legal grounds for the entire terrestrial fleet with respect to CO₂ emissions no matter the propulsion fuel (gas or diesel) [11, 12].

It can be concluded that research in this field is an ongoing process and still raises a series of new challenges. The complexity of the manufacturing processes and the high amounts of material loss generated, as well as the limited capacities of obtaining complex geometries with multi-functional capabilities represent only a part of these current challenges. The main objective of extending research in the field of advanced lightweight cellular structures is to develop new solutions with high structural performances together with simple production technologies which could ensure overall cost reduction.

1.2 Types of cellular cores used for the construction of sandwich panels

The topology of the cellular cores used in the construction of sandwich panels can be divided into two main categories: *i*) periodic cellular structures and *ii*) stochastic cellular structures.

1.2.1 Periodic cellular structures

The main advantage provided by periodic cellular structures is that their structural performance is directly influenced by the properties of the base material. In this regard, they can be maximally exploited through the topology of the unit cell. They are usually designed using plate or truss-like elements and can be classified as follows.

■ *Periodic cellular cores with open or closed topology*

Periodic cellular cores with open topologies and continuous channels are used in applications which require good shock absorption capabilities and effective heat exchange while maintaining a reduced height [13, 14, 15].

Periodic closed-cell corrugations represent a variation of open cell core with a supplementary step added within the manufacturing process. This consists in bonding several strips of corrugated panel using assembling methods like adhesive, brazing, spot welding etc. [16, 17].

■ *Lattice truss cellular cores*

Lattice-truss cellular cores are of considerable interest for the advanced lightweight materials industry due to their high strength-to-weight ratio and multifunctional potential provided by the open-space geometry. They have been successfully used in the aerospace and automotive industry [18].

Lattice-truss structures usually consist in filled or hollow trusses with circular or rectangular sections which are then formed into different topologies: tetrahedral, pyramidal, double-layered pyramidal etc.

The mechanical performance of sandwich panels based on periodic cellular cores are defined by the stiffness and strength under different loading scenarios and boundary conditions. When designing cellular cores with complex topologies it is imperative to take into consideration the Poisson's ratio of

the structure. Also known as transverse contraction coefficient and defined as the ratio between the resulting deformation on the direction perpendicular to the acting load and the deformation in the loading direction it has a significant influence on the mechanical properties of the cellular core.

The Poisson's ratios of a cellular structure can be divided into three main categories: a) positive; b) zero; c) negative [19, 20, 21, 22].

Cellular structures with positive Poisson's ratio exert a transverse contraction in tensile loading and extension in compression loading [23, 24].

Structures with negative Poisson's ratio, also known as auxetic structures, are characterised by lateral contraction when subjected to compression loading and expansion in the direction of the tensile loading [25].

A special category of behaviour is represented by structures whose Poisson's ratio is equal to zero, which means that there is no transverse deformation when the structure is subjected to tensile or compression loading.

The last two categories are usually represented by cellular optimisations of the honeycomb core and are successfully used in the aerospace, bio-medical, naval, and automotive industries.

1.2.2 Stochastic cellular structures

Foam cellular cores are used in the construction of sandwich panels due to their low relative density together with a high potential for absorbing impact energy. Having high stiffness and strength, fatigue resistance and acoustic damping, they have been successfully used in wind turbine blades and several transportation applications [26, 27, 28].

Stochastic foams can be divided into two main categories: *i*) metallic, and *ii*) non-metallic.

1.2.3 Hierarchical cellular structures

Structural hierarchy, inspired by natural materials (bone, wood etc.) has become a practical solution when it comes to the design of cellular structures. Thus, the hierarchical sandwich panel now represents a special category for which the core of a sandwich assembly is represented by a sandwich panel itself.

The technique of structural hierarchy of cellular cores is relatively accessible with respect to production technologies and indicates potential for design and construction of high-efficiency multifunctional cores. From the many advantages highlighted by existing research high energy absorption capabilities and thermal and acoustic insulation are the most notable ones [29, 30, 31]. From the structural performance point of view, hierarchical cores have a higher stiffness and buckling strength when subjected to mechanical loading (compression, shear, bending) as opposed to the first order structures from which they are derived [32, 33].

1.3 Materials and technologies used in the construction of sandwich panels

The materials used in the construction of sandwich panels can be synthesized into two main categories, in terms of the element which they are referred to: *i*) materials used for the face sheets and *ii*) materials used for the core, as presented below.

In terms of mechanical properties, they have to fulfil several requirements: *i*) high buckling and bending strength, *ii*) high compression, tension and impact stiffness, *iii*) high wear capacities [18, 34, 35].

When discussing the production of face sheets for sandwich panels, the most used materials are metallic alloys (e.g. aluminium and steel alloys) due to their good quality-price ratio.

1.3.1 Materials and technologies used for the fabrication of the face sheets

Metallic sandwich face sheets are obtained through a simple cold forming process. The metal block is turned into thin plates by passing through two revolving cylinders followed by a cutting process at the desired dimension of the panel [35].

The demand for materials with high mechanical properties has led to the implementation of several lightweight materials into mass production such as: reinforced plastics based on carbon and glass fibres (with random or pre-set orientation), memory alloys and ceramic composites, with the purpose of reducing the mass of mechanical assemblies. They are the most cost-effective materials to provide high strength-to-weight ratio as well as considerable energy absorption capacities [36,37].

The manufacturing processes of composite materials are more complex and involve higher costs as opposed to metallic sheets; they are not entirely automated and often include a series of manual operations, which may lead to manual errors.

They often include the use of a positive-negative die, previously treated with a coating layer, for an easy release of the part from the mould. Subsequently, a topcoat is added, which will represent the finished surface of the part. This step is used to ensure specific roughness of the outer surface for different applications. The actual manufacturing process consists in applying successive layers of carbon fibre weave and epoxy resin coatings. Once the layup is finished, the dye is cured in a hot air oven or vacuum press at a specific temperature for a fixed amount of time as specified in the data sheet [38].

Another category of materials with high perspectives for large scale use in the construction of sandwich panel is represented by intelligent materials [39, 40, 41].

Intelligent materials can change their behaviour and mechanical properties according to the action exerted on them by different stimuli. They are divided into two main categories: *i*) shape memory alloys – the shape of the part is pre-set during the manufacturing process to which the structure could return when exposed to high temperatures; *ii*) shape morphing materials - structures which can change their shape during functioning when exposed to outside stimuli [42, 43].

Even though the use of carbon fibre reinforced materials has increased, mainly due to their low density, high stiffness and strength, long lifecycle etc., their main drawback which continues to raise issues is the low recyclability capabilities, thus when the end of lifecycle is reached they are usually stored in waste compounds or send to landfills. Since this is not a benefit for the environment, alternatives are continuously being developed [42, 44, 45].

In this regard, another category of composite materials has emerged - natural fibres reinforced plastics. These are polymer-based matrixes reinforced with natural fibres, such as: hemp, coconut, flax etc. and are usually taken into consideration when designing composite materials due to their high recycling capacity [46].

The mass production of natural fibres composites has reached 400.000 tonnes annually. Manufacturers have taken up the use of natural composites due to three main advantages: *i*) high strength-to-weight ratio as opposed to low CO₂ emissions, *ii*) biodegradability and *iii*) high renewal abilities [47, 48, 49, 50].

Although research conducted up to the present in the industry of advanced lightweight materials, supported by the multitude of existing solutions with high mechanical performances, metal alloys remains the norm due to reduced manufacturing costs (material usage and technologies) with respect to good mechanical performances.

1.3.2 Materials and technologies used for the construction of cellular cores

The main purpose of the cellular core within the sandwich assembly is to keep a constant distance between the face sheets. In additions to this, it still has to provide other structural requirements, such as: low relative density, high out-of-plane stiffness and considerable shear stiffness.

The materials used for the construction of cellular cores can be divided into two main categories:

- Metallic materials – metal alloys based on aluminium, titanium, nickel, copper
- Non-metallic materials – wood, paper, resin saturated paper etc. [1, 2].

Despite the wide range of available materials for the construction of cellular cores, metallic alloys remain still the best prospect. They are successfully used in industrial applications due to their high strength-to-weight and quality-price ratios.

Metallic cellular cores can be obtained through different technological processes, as follows.

■ *Mechanical expansion*

Cellular cores manufactured through a mechanical expansion process require the use of multiple thin metallic sheets cut at the same bulk dimensions. Subsequently, they are glued together on the longitudinal direction and dispersed at a pre-set dimension. The resulting sheet metal stack is then cut at the desired dimension which will become the height of the cellular core. Later, they are mechanically expanded by applying a load on the direction perpendicular to the glue application. This is maintained until the unit cells become of a desired shape and size [35, 36].

■ *Cold forming*

Cellular structures with open or closed topologies can also be obtained through a cold forming process, where a thin sheet metal is pressed in a negative-positive die with the shape of the desired profile (triangular, square, sinusoidal, trapezoidal, etc.). The resulting corrugated profile is then cut at the desired dimensions, and can be used as a core in the construction of sandwich panels [35].

■ *Thermal forming*

From the category of non-metals for the construction of cellular cores, thermoplastic materials are the most extensively used. These are obtained in heated negative-positive presses from thin plastic sheets. The plastic sheet is placed in a cooled press which is then pre-set to the desired temperature. When this is reached, the top press is displaced vertically at a constant speed to create the desired shape of the corrugation [38, 52].

■ *Additive manufacturing*

Additive manufacturing technology (previously known as 'rapid prototyping') has emerged in the beginning of the 1990s and provides the possibility of obtaining cellular structures by eliminating material loss. This technology uses different types of materials such as: liquids, powders (e.g. ceramic powders) and solids (e.g. ABS).

The part is generated in its 3D shape using the CAD model (previously designed in specific software) by adding successive thin material layers on a support plate, process also known as 3D lamination.

Cellular cores for the construction of sandwich panels obtained by additive manufacturing can be obtained from a wide range of thermoplastic materials, metallic or ceramic. They present good quality of impact energy absorption. Nonetheless, this manufacturing method is not cost efficient and thus, not suitable for mass production [53, 54].

■ *Weaving of metallic wires*

Another method of obtaining periodic cellular cores is represented by the weaving of continuous metallic wires with hollow circular section. This procedure results in obtaining an open cellular structure which can be used in the construction of sandwich panels. These types of structures offer the advantage of being cheap to obtain and provide high lightweight capabilities [55, 56, 57].

■ *Folding techniques*

A relatively new category proposed by the scientific community working on developing cellular cores for the construction of sandwich panels is represented by structures obtained through different folding techniques. This method consists in folding a flat thin sheet after a pre-set pattern and provides the advantage of obtaining various tri-dimensional cellular structures (3D) [58, 59, 60].

1.4 Critical analysis of the state of the art

Natural structures remain up to the present an endless source of inspiration for the development of sandwich cores and offer a multitude of solutions in order to counteract the existing design problems researchers are dealing with. This inspiration has led to the design of the honeycomb core, Figure 1.2, which is considered the state-of-the-art in the field of lightweight cellular cores and it is extensively used since its design up to the present, especially in the aerospace industry [61, 62].

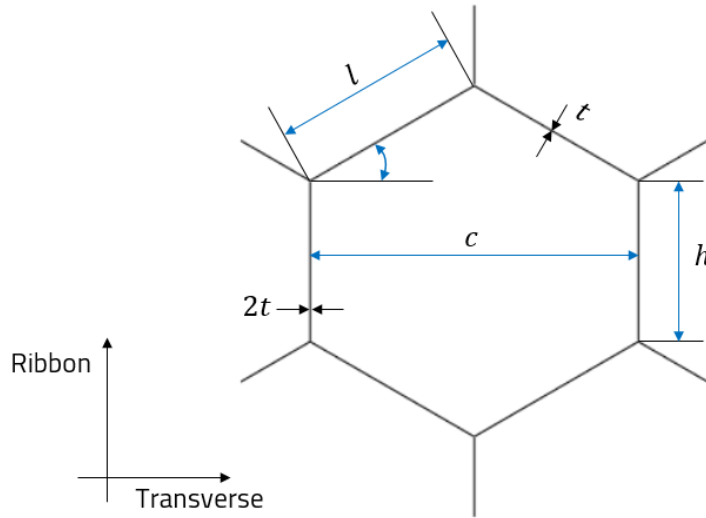


Figure 1.2 Parametric unit cell of the honeycomb cellular core [62]

The large-scale use of this cellular core is due to its remarkable strength-to-weight properties. Amongst the multitude of advantages it provides, it is worth mentioning good thermal insulation, heat transfer, impact energy absorption etc. [62, 63].

Even though honeycomb-based sandwich structures are the most common choice, when it comes to high performance applications their disadvantages are not to be neglected. Worth mentioning are core crushing, shear and buckling. In addition to this, they trap moisture, due to their closed-cell structure, which may lead to internal corrosion and face sheet de-bonding [64, 65].

Adhesion surface also plays an important role in the assembling process of a sandwich panel. For honeycomb core-based panels, this surface is equal to the thickness of the base material (double the thickness on some regions) which brings additional requirements on the manufacturing process and, thus, significantly increasing the production cost [66, 67, 68, 69].

To address the disadvantages of the classic honeycomb structure, researchers have proposed a wide range of cellular topologies for simplifying the technological manufacturing processes while offering competitive mechanical properties. Thus, low-density cellular cores have been developed as an alternative solution to the honeycomb, depending on the targeted application [70].

Truss-like lattice structures are of considerable interest for the industry of advanced lightweight materials due to their high stiffness and strength to weight ratios and their multifunctional potential due to their open-cell geometries. Another advantage of lattice structures in the sandwich core is the possibility of being formed into numerous core topologies due to their high geometric versatility. The sandwich face sheets are added either through brazing, welding or through bonding with different types of adhesives [71, 72].

Despite their good compression properties, lattice structures often show signs of failure of the assembling method when subjected to shear loading. The bonding method of the face sheets makes the sandwich panel susceptible to premature failure. Nonetheless, this is a general aspect of lattice truss corrugations for which manufacturing methods are flawed and are also not attractive for bulk and mass production. Within this context, the following conclusions can be drawn.

1.5 Conclusions of the state-of-the-art review

After performing the critical review of the state of the art on the advanced lightweight structures with respect to the status of the development, design and investigation of sandwich panel construction, the following conclusions can be drawn:

- The demand for high-performance structures has led to continuous development of the advanced lightweight structures industry.
- For the design and construction of sandwich panels, a multitude of existent materials can be considered (metallic or non-metallic) but the most used are the ones whose manufacturing technologies remain simple and cost efficient.
- Cellular cores have to meet a series of strict requirements. The most important are represented by: low density, high strength and stiffness both for in-plane and out-of-plane loading, high impact energy absorption, thermal and acoustic insulation.
- The intention is to develop solutions which allow obtaining complex and performant structures which should ensure cost and material reduction, simple manufacturing processes, significant adhesion surfaces and easy assembling techniques.
- There are still some challenges which remain up to date at this moment: *i)* inability to obtain complex geometries and *ii)* simplifying the manufacturing technologies and reducing overall costs. This ensures the continuous possibility of developing new cellular architectures which may address the disadvantages highlighted by the present study.

2. Research goals and objectives

The present research consists in the study of the topology, behaviour and mechanical properties of a novel pyramidal cellular structure obtained through a mechanical expansion process which has to meet the following requirements:

- high structural performance in different loading scenarios;
- weight reduction of the associated assembly.

To achieve the main goal of this doctoral thesis, the following objectives have been set:

1. Critical review of the state-of-the-art in the field of lightweight advanced structures;
2. Study of the novel pyramidal structure to be used as core in the construction of sandwich panels
 - topologic study of the periodic cellular structure;
 - material choice and study on the manufacturing method of the corrugated core.
3. Theoretical analysis of the novel structure under study
 - developing the analytical model of the pyramidal structure's unit cell;
 - developing the numerical model of the sandwich panel based on the novel cellular core.
4. Experimental testing of the structure for both the isolated unit cell of the corrugation as well as of the associated sandwich panel.
 - creating the samples for the experimental model;
 - subjecting the samples to experimental testing, collecting the data, and analysing the results.
5. Validation of theoretical models based on their correlation with experimental data.

3. Study of the novel pyramidal cellular structure for the construction of sandwich panels

3.1 Novel pyramidal cellular structure and its manufacturing principle

Inspired by natural structures, the honeycomb core became the state-of-the art cellular structure in this field. Although honeycomb-based sandwich panels exhibit outstanding mechanical performances, the manufacturing process remains complex, and the costs are high.

In this regard, a novel pyramidal cellular core designed by Marian N. Velea throughout his research work at the Transilvania University of Brașov is proposed for investigation. Obtained through a simple manufacturing process, with reduced material loss, it represents a potential a solution to address the afore mentioned disadvantage.

The pyramidal cellular structure derives from a perforated trapezoidal corrugation, with an additional internal angle A , as it is shown in Figure 3.1.

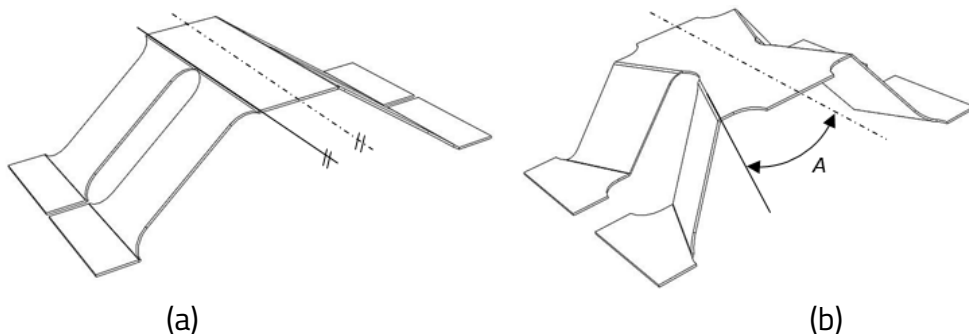


Figure 3.1 Schematic representation of the cellular structure: a) perforated trapezoidal corrugation; b) mechanically expanded perforated trapezoidal corrugation resulting in a pyramidal structure [73].

The cellular core can be obtained from a thin sheet of any type of ductile metal (e.g. aluminium alloys, stainless steels etc.), through a continuous manufacturing process, Figure 3.2.

The manufacturing technique, described as mechanical expansion, is performed by following a few simple steps: *Perforation* → *Generating the guiding lines (bends)* → *Mechanical expansion*.

A pattern of perforations is generated on a flat metal sheet. This results in a profile numbered 1, 2 (zone I). Successively, a series of bends, numbered 3, is generated onto the perforated profile to better control the expansion process (zone II). These bending lines form the internal angle of the structure, A . Finally, the perforated metallic profile is fixed at one end (points O_1 and O_2) while at the opposite end a specific displacement U_x is applied along the direction of expansion. The process is stopped when the cells reach the desired bulk dimensions [73].

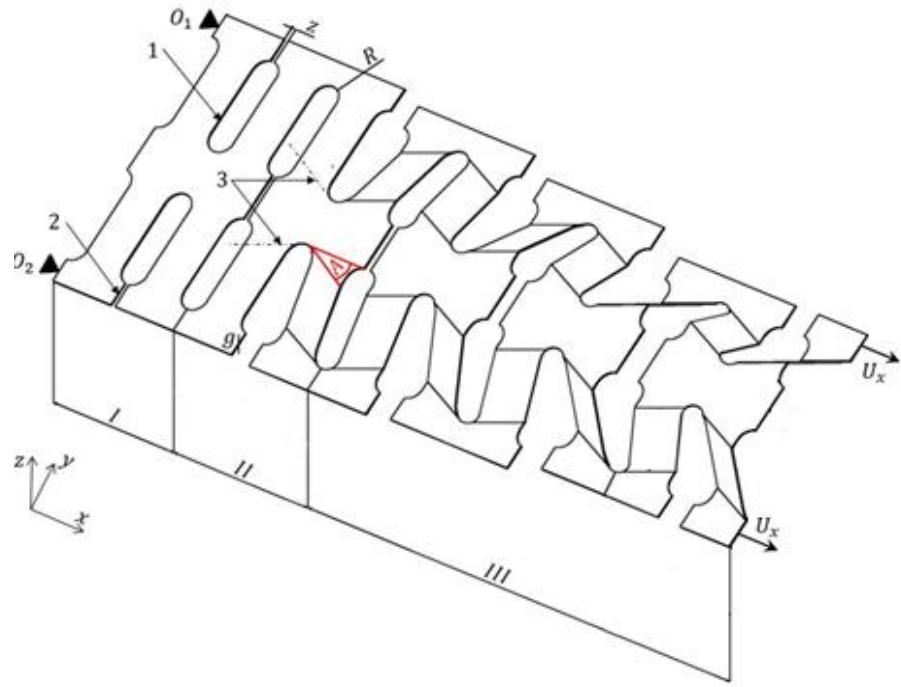
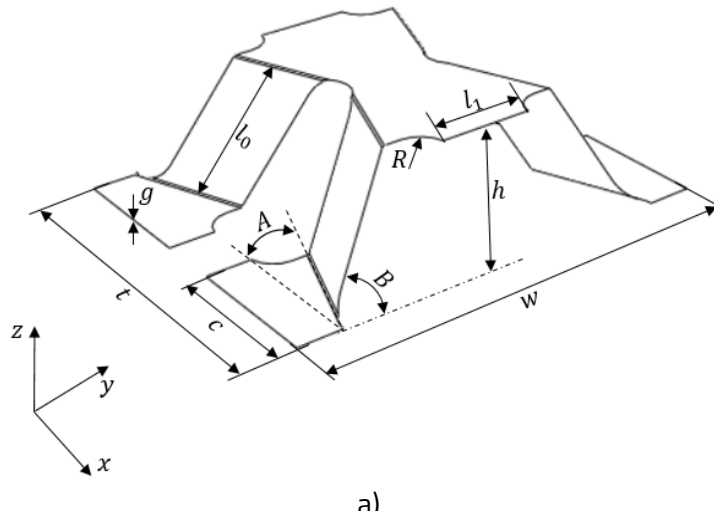


Figure 3.2 Key steps in the manufacturing process of the pyramidal cellular structure [73].

The result of this manufacturing process is represented by a bi-directional pyramidal corrugated structure expanded on both Ox , Figure 3.3 b) and Oy axes, Figure 3.3 c). Considering the placement of the cellular core between the face sheets, two different configurations can be obtained by mirroring the unit cell in the XZ and YZ planes, Figure 3.3 a).



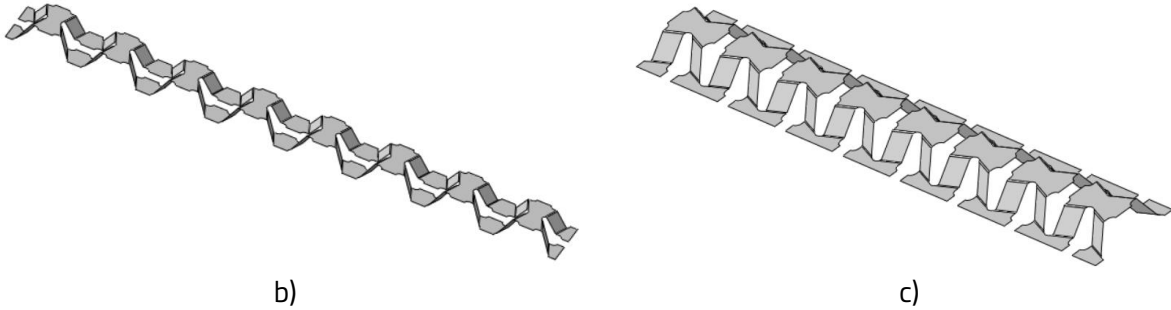


Figure 3.3 The schematic representation of the pyramidal cellular core: a) the unit cell and its parameters; b) the resulting core expanded on the O_x direction; c) the resulting core expanded on the O_y direction [74].

3.2 Parametric study of the cellular topology

For the parametric study of the novel pyramidal cellular core, the representing unit cell has been identified on which the following geometric parameters have been defined, Figure 3.3 a):

c – base of the cell's arm, z – thickness of the cutting tool, R – radius of the perforation, g – thickness of the base material, A – internal angle of the structure, t – width of the expanded structure, l_0 – length of the strut, l_1 – distance between the perforations, h – height of the expanded unit cell, B – inclination angle of the strut, w – length of the expanded unit cell.

The internal angle of the structure, A , represents the novelty this pyramidal structure brings. Defined by a tangent axis between two consecutive circular perforations; it can be computed using equation (3.1).

$$A = \arctan\left(\frac{2 \cdot R}{c}\right), \quad (3.1)$$

Based on the computation relation of the expansion angle and taking into consideration the other geometrical parameters defined on the unit cell, the length (w), width (t) and height (h) of the unit cell are defined [73]:

$$w = 2 \cdot l_1 + 2 \cdot l_0 \cdot \cos(B) + c \cdot \tan(A) + 2 \cdot R, \quad (3.2)$$

$$t = 2 \cdot c + z + l_0 \cdot \sin(B) \cdot \tan(A), \quad (3.3)$$

$$h = 2 \cdot g + l_0 \cdot \sin(B), \quad (3.4)$$

where: z is the thickness of the cutting tool, Figure 3.2.

Computing the relative density, ρ_r , of a corrugated core is the most effective way to evaluate its lightweight characteristics. The relative density is defined as the ratio between the volume of base material (V_m) of the cellular core is manufactured and the volume of the resulting structure (V_s) [74].

$$\rho_r = \frac{V_m}{V_s}, \quad (3.5)$$

The relative density of the pyramidal cellular core under study is computed using equation (3.6).

$$\rho_r = \frac{4 \cdot c \cdot g(l_0 + l_1 + 2 \cdot R) - z \cdot g \cdot l_1 - 8 \cdot g \cdot l_0 \cdot R - 4 \cdot \pi \cdot g \cdot R^2}{w \cdot t \cdot h}, \quad (3.6)$$

By defining the equations for the bulk dimensions of the unit cell, w , t , and h as well as the relations for the relative density, ρ_r , performing a parametric study is now possible. Its purpose is to analyse the variation of the geometric parameters of the unit cell with respect to the manufacturing process.

For the parametric study, the configurations were obtained with the help of two sets of parameters: one of fixed parameters - including the distance between two consecutive perforations, l_1 , the base of the cell's arm, c , thickness of the cutting tool, z and thickness of the base material, g and one of variable parameters - including the length of the strut, l_0 and the radius of the perforation, R .

The algorithm used to design the configurations proposed for the parametric study is shown in Figure 3.4.

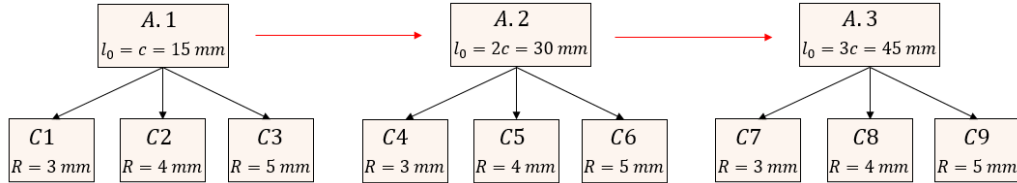


Figure 3.4 The algorithm for forming the configurations subjected to the parametric study.

With respect to the values of the defining parameters, the variation of the unit cell's length and width, computed with the help of equation (3.2) and (3.3) respectively, is depicted in Figure 3.5. The value for the length of the unit cell is indirectly proportional with the increase of the inclination angle of the struts. This behaviour is similar for all the configurations considered throughout the study.

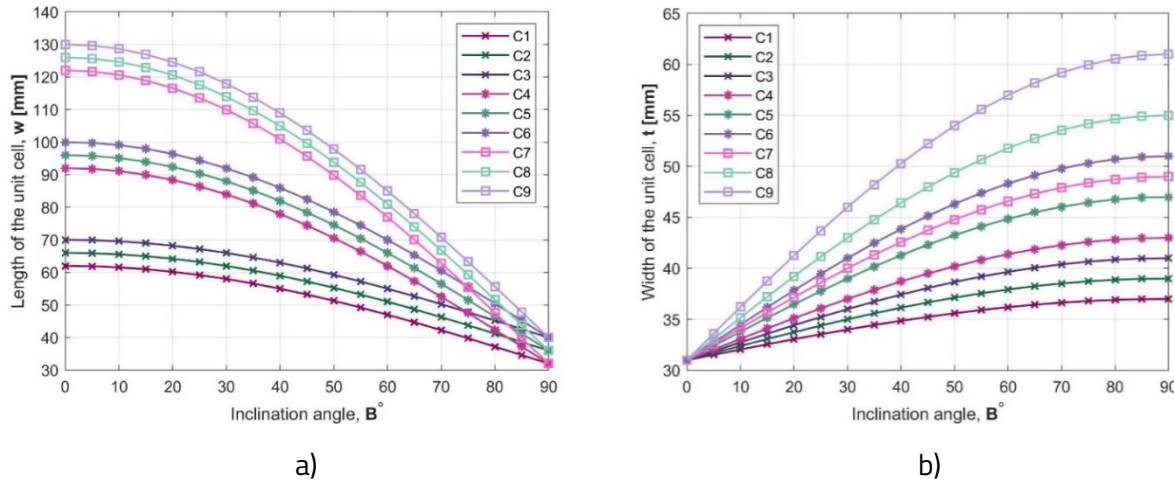


Figure 3.5 The variation of: a) the length of the unit cell; b) the width of the unit cell with respect to the inclination angle of the strut.

On the other hand, the relation between the variation of the inclination angle and the change in value of the width of unit cell, defined by equation (3.3), has the opposite behaviour. It increases directly proportional with an increase in value of the inclination angle, Figure 3.5.

When discussing the evolution of the unit cell's height, defined by equation (3.4), in respect to the inclination angle of the strut, two conclusions can be drawn: *i*) a directly proportional increase in height is registered together with the increase of the inclination angle; *ii*) the height is the same in the case of the three sub-configurations, since it is defined only with respect to the angle in question, Figure 3.6.

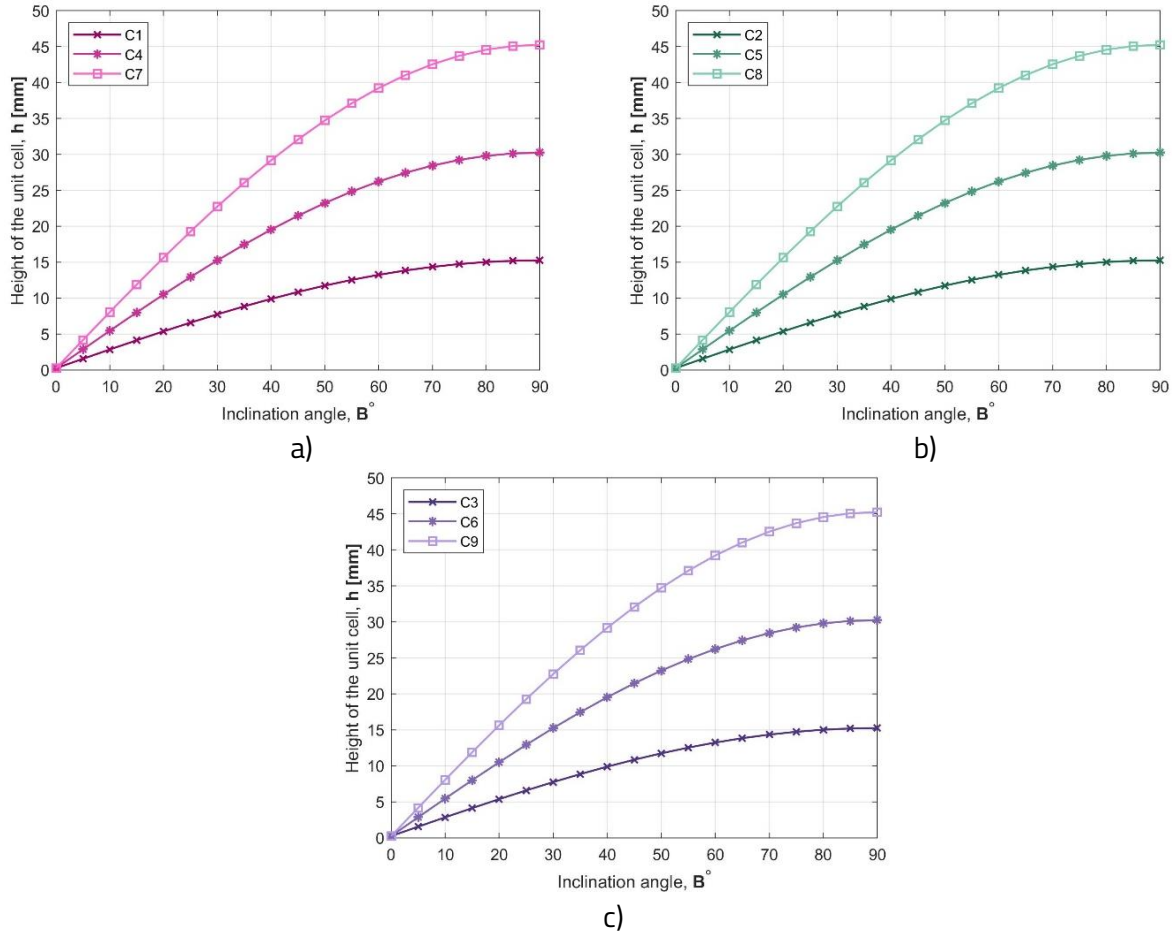


Figure 3.6 The variation of the height of the unit cell with respect to the inclination angle of the strut: a) $R = 3$ mm; b) $R = 4$ mm; c) $R = 5$ mm.

The graphs depicted in Figure 3.7, define the variation of the relative density with respect to the inclination angle of the strut. The relative density decreases in value together with an increase of the inclination angle of the strut. A significant drop in value is registered when the inclination angle reaches 5° . After this point the value for the relative density is constantly maintained under 0.1. The minimum is recorded when $B = 50^\circ$ but, despite this, the variation is approximately linear in the range of $[40^\circ - 70^\circ]$.

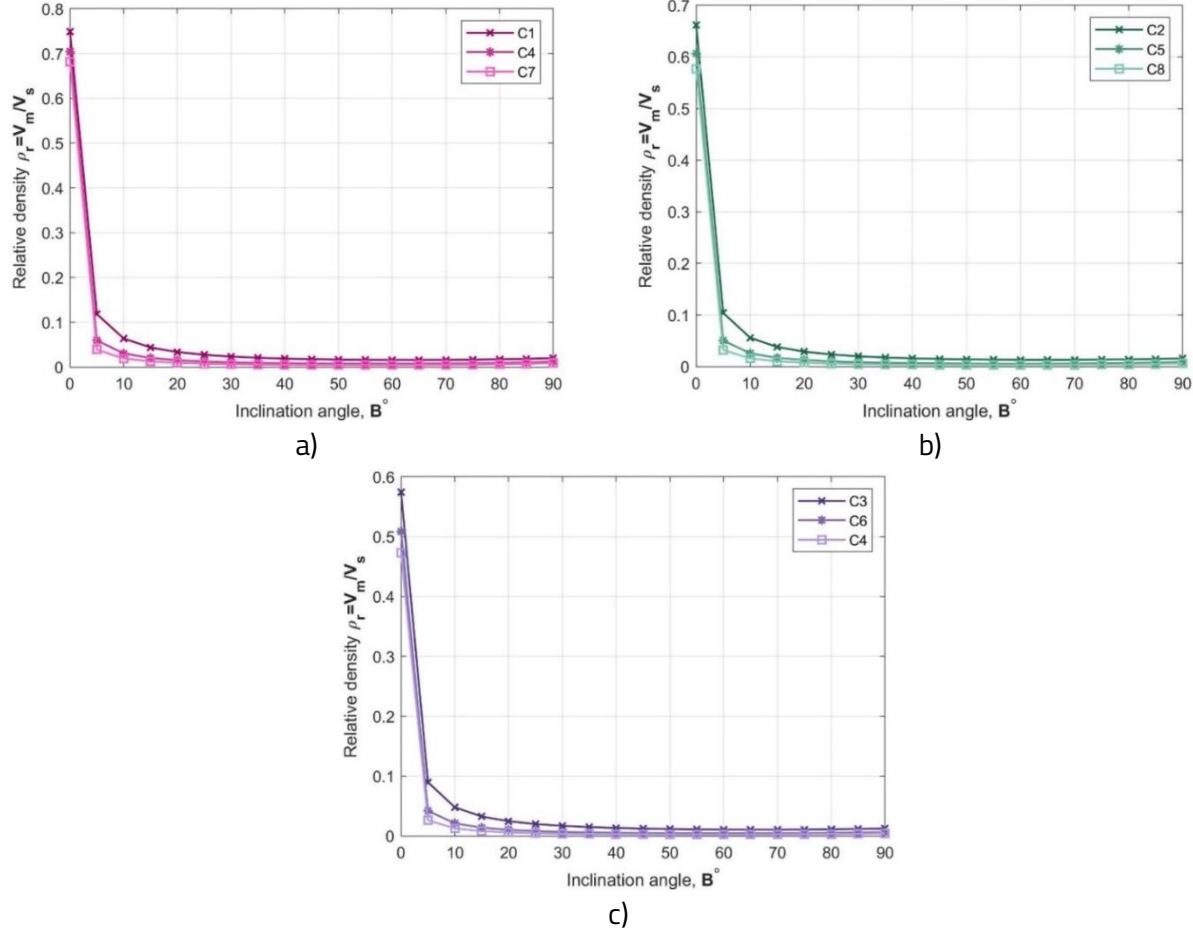


Figure 3.7 The variation of the relative density of the unit cell with respect to the inclination angle of the strut: a) $R = 3 \text{ mm}$; b) $R = 4 \text{ mm}$; c) $R = 5 \text{ mm}$.

3.3 Trapezoidal cellular structure

Due to the topology of the structure, the internal angle of the structure, A , can take values in the range $A = [0, \arctan(2 \cdot R/c)]$. The upper limit of this interval leads to obtaining the pyramidal structure defined in Figure 3.3 b) while the lower limit defines a trapezoidal cellular structure, Figure 3.3 a).

For the trapezoidal core, based on the metallic perforated profile, the value of internal angle of the structure, A , is equal to zero, Figure 3.8.

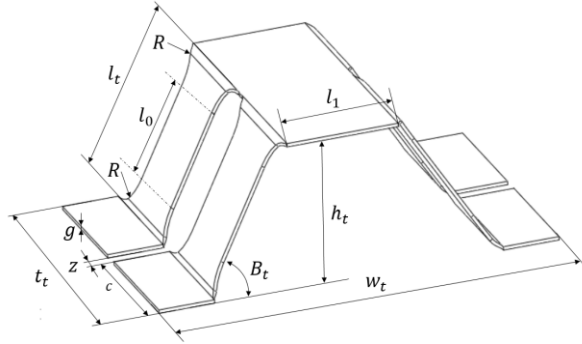


Figure 3.8 The schematic representation of the trapezoidal cellular core and its parameters.

With respect to the trapezoidal topology, the geometric parameters defining the unit cell are as follows:

c – base of the cell's arm, **z** – thickness of the cutting tool, **R** – radius of the perforation, **g** – thickness of the base material, **t_t** – width of the expanded structure, **l_t** – length of the strut, **l₁** – distance between the perforations, **h_t** – height of the expanded unit cell, **B_t** – inclination angle of the strut, **w_t** – length of the expanded unit cell.

Based on the computation relation of the bulk parameters of the pyramidal unit cell, equations (3.2), (3.3) and (3.4) and taking into consideration that for the trapezoidal corrugation $A = 0$, the length (w_t), width (t_t) and height (h_t) of the unit cell can be defined:

$$w_t = 2 \cdot l_1 + 2 \cdot l_t \cdot \cos(B_t), \quad (3.7)$$

$$t_t = 2 \cdot c + z, \quad (3.8)$$

$$h_t = 2 \cdot g + l_t \cdot \sin(B_t), \quad (3.9)$$

where: z is the thickness of the cutting tool;

The relation between the length of the strut for the two studied configurations, l_0 and l_t , is defined with the help of the equation below:

$$l_t = l_0 + 2 \cdot R, \quad (3.10)$$

The value for the length of the unit cell is indirectly proportional with the increase of the inclination angle of the struts, which means that the length of the unit cell decreases together with an increase of the inclination angle. This behaviour is similar for all the configurations considered throughout the study, Figure 3.9 a).

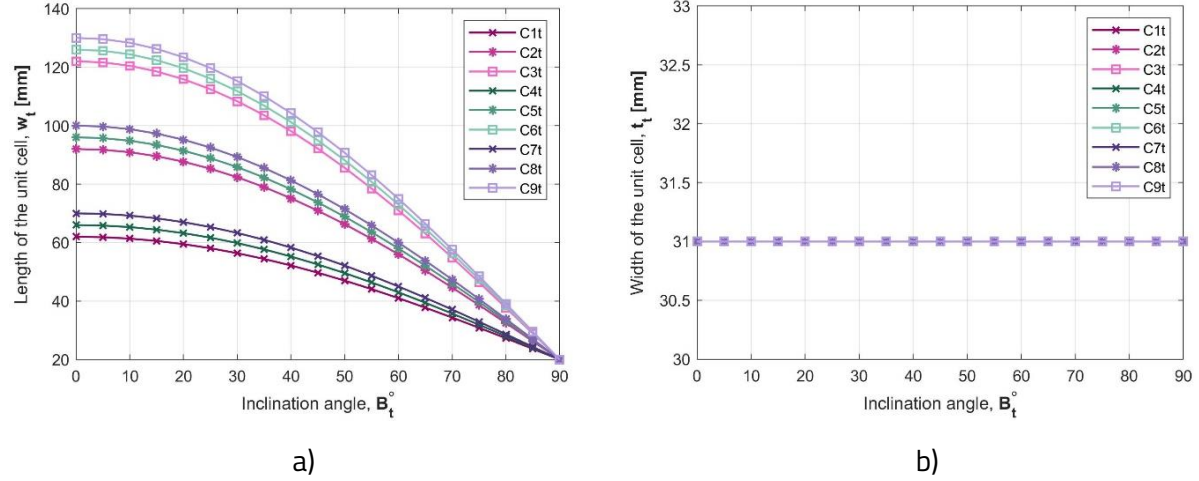
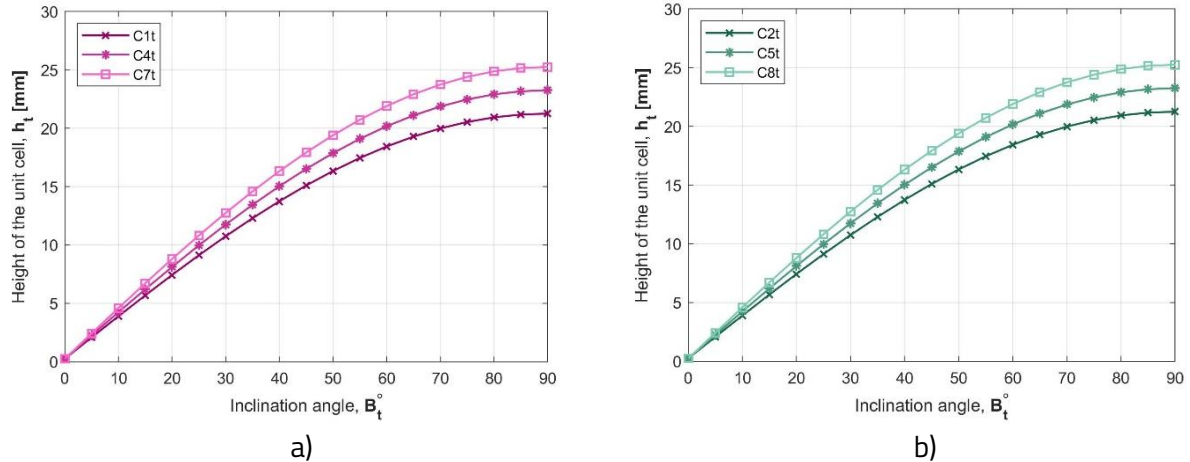
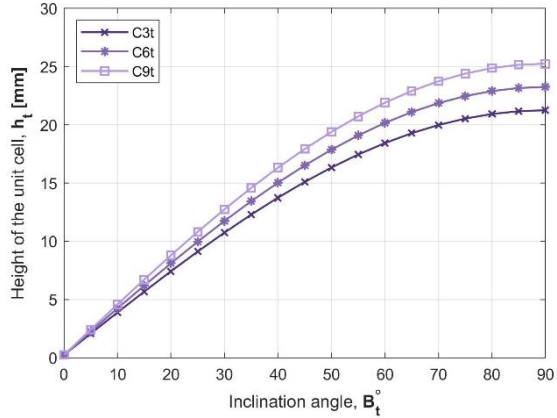


Figure 3.9 The variation of: a) the length of the unit cell; b) the width of the unit cell with respect to the inclination angle of the strut.

On the other hand, the relation between the variation of the inclination angle and the value of the width of unit cell, defined by equation (3.8) is linear. Since the trapezoidal structure has no internal angle, the width of the unit cell is the same for all the investigated configurations, $t_t = 31$ mm, Figure 3.9 b).

The evolution of the unit cell's height, defined by equation (3.9), in respect to the inclination angle of the strut has a directly proportional increase together with the increase of the inclination angle. The height is the same in the case of all the investigated configurations, since it is defined only with respect to the angle in question, Figure 3.10.



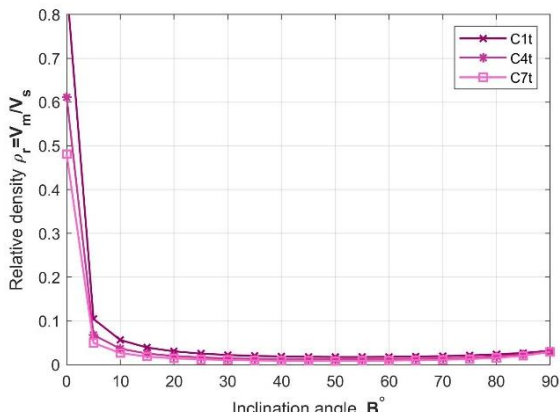


c)

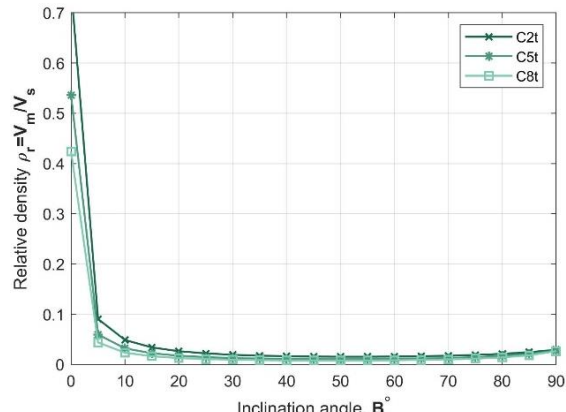
Figure 3.10 The variation of the height of the unit cell with respect to the inclination angle of the strut: a) $R = 3\text{ mm}$; b) $R = 4\text{ mm}$; c) $R = 5\text{ mm}$.

Both the width and height of the unit cell have the same behaviour with respect to the inclination angle. They both increase together with the increase of the afore mentioned angle. The effect is different when the length of the unit cell is considered, this is the same for all the configurations subjected to study. Since the topology of the trapezoidal structure does not account for the internal angle, the expansion of the unit cell is only on the x and z axes.

The graphs depicted in Figures 3.11, define the variation of the relative density with respect to the inclination angle of the strut. The relative density decreases in value together with an increase of the inclination angle of the strut. A significant drop in value is registered when the inclination angle reaches 5° . After this point the value for the relative density is constantly maintained under 0.1. The minimum is recorded when $B = 50^\circ$ but, despite this, the variation is approximately linear in the range of $[45^\circ - 65^\circ]$.



a)



b)

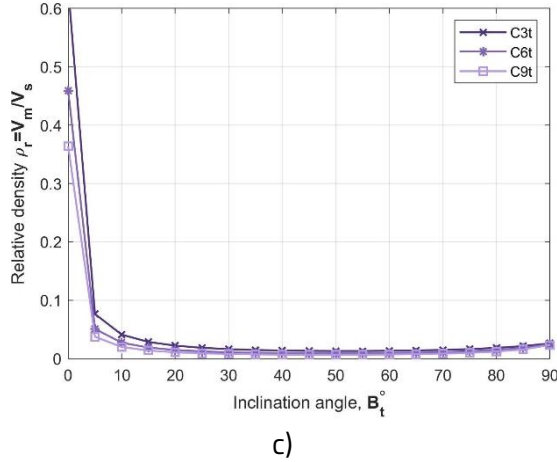


Figure 3.11 The variation of the relative density of the unit cell with respect to the inclination angle of the strut: a) $R = 3\text{ mm}$; b) $R = 4\text{ mm}$; c) $R = 5\text{ mm}$.

The variation of the relative density is similar for all the configurations subjected to study and is maintained at considerably low levels.

The comparison between the effective density of the trapezoidal structure as opposed to the pyramidal one, for an inclination angle of the strut, $B = 60^\circ$, are presented in Table 3.1.

Table 3.1 Comparison of effective density between the two topologies, pyramidal and trapezoidal

Density [kg/m^3] (configuration)		Difference [%]
$\rho_{C_1} = 126.16$	$\rho_{C_{1t}} = 140.49$	10.2
$\rho_{C_2} = 104.48$	$\rho_{C_{2t}} = 123.35$	15.3
$\rho_{C_3} = 85.19$	$\rho_{C_{3t}} = 105.8$	19.5
$\rho_{C_4} = 58.93$	$\rho_{C_{4t}} = 98.31$	40
$\rho_{C_5} = 45.9$	$\rho_{C_{5t}} = 86.86$	47.1
$\rho_{C_6} = 35.07$	$\rho_{C_{6t}} = 74.85$	53.1
$\rho_{C_7} = 36.2$	$\rho_{C_{7t}} = 74.52$	51.4
$\rho_{C_8} = 27.07$	$\rho_{C_{8t}} = 65.94$	58.9
$\rho_{C_9} = 19.81$	$\rho_{C_{9t}} = 56.85$	65.1

The comparative study between the two investigated structures has shown that the pyramidal core has considerably better lightweight capabilities as opposed to the trapezoidal one, thus proving that the presence of the internal angle represents an advantage of the novel pyramidal structure. In this regard, an investigation on the mechanical properties would be the next step of this research.

3.4 Comparative study

The performance of the pyramidal cellular structure under investigation has been determined by conducting a study between some of the most common solutions proposed as cores for the design and construction of sandwich panels was performed. Four topologies have been considered, which were already defined in the literature regarding relative density [75, 76]: triangular, trapezoidal, honeycomb and ExpaAsym, Figure 3.12.

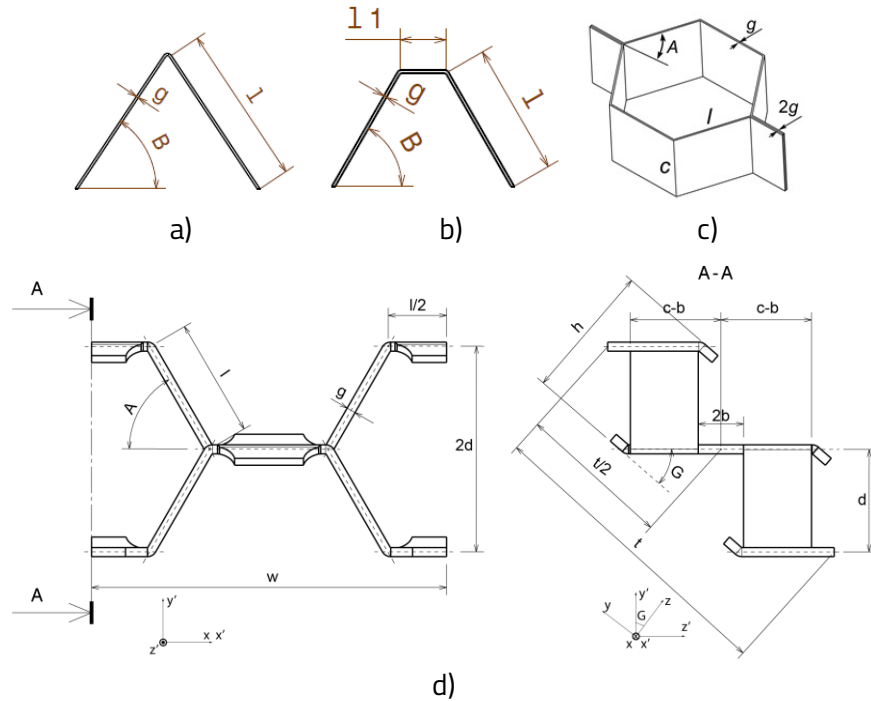


Figure 3.12 Main core topologies for sandwich panel construction: a) triangular; b) trapezoidal; c) honeycomb; d) ExpaAsym [76].

Several relations between the defined parameters were maintained in order generate a valid comparison and to highlight the advantages of the newly developed cellular structure. The length of the strut, (l) has been kept constant for all of the corrugations mentioned above, $l = [15, 30, 45]$. The expansion angle was varied in the range $[0^\circ - 90^\circ]$ according to how permissively the topology of the corrugations is. The width, (t) and the height, (h) were determined in respect to the length of the unit cell, (w) with the help of the following relations: $t = w/2$ for the triangular and trapezoidal cores and $h = w/2$ for the honeycomb core.

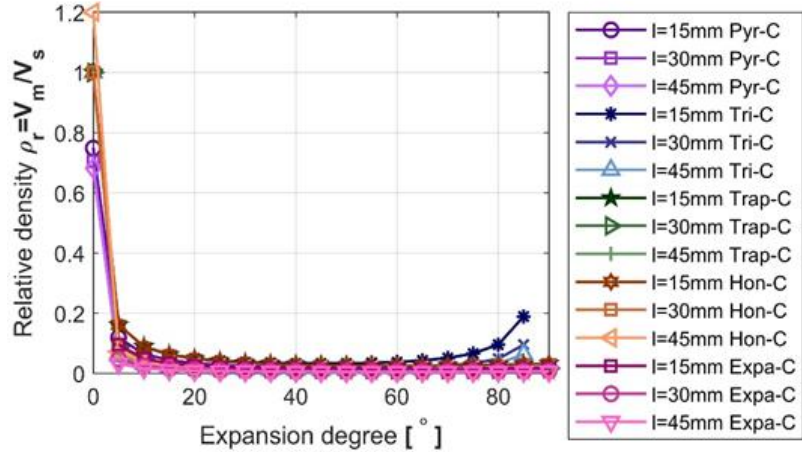


Figure 3.13 The evolution of the relative density with respect to the expansion degree for the studied topologies [76].

The evolution of the relative density with respect to the expansion degree is depicted in Figure 3.13, where: Pyr-C – studied pyramidal cellular core, Tri-C – triangular cellular core, Trap-C – trapezoidal cellular core, Hon-C – honeycomb cellular core, Expa-C – ExpaAsym cellular core [76, 77, 78, 79].

The graph shows that the relative density has a similar evolution for all the studied corrugations, in all the specified configurations; it decreases when increasing the expansion degree. The minimal values are registered in the range $[30^\circ - 70^\circ]$, depicted in Figure 3.13. It is worth mentioning that the relative density decreases together with the increase of the unit cell's strut, since it generates a higher volume of void in the cellular structure. Thus, the maximum values registered were in the case where $l = 15 \text{ mm}$, while the minimum ones were encountered for $l = 45 \text{ mm}$.

The relative density of the triangular topology registers values in the range $[0.01-0.04]$, while for the trapezoidal structure, these are set between $[0.015-0.035]$, with the advantage that the latter provides a significant adhesion surface, which could deliver a more cost-efficient manufacturing process.

In comparison to the trapezoidal corrugation, the relative density of the honeycomb cellular core has the same evolution, with identical values, in the given range of $[0.015-0.035]$. This is because the honeycomb core represents a closed topology consisting in two trapezoidal structures bonded to each other, but the bonding surface provided by the honeycomb core is reduced; it is equal to the thickness of the base material, and, in some cases, it can be doubled, which could lead to premature failure of the bonding mechanism. Despite this, it is successfully used in many applications where high mechanical properties are required (strength, stiffness, high impact energy absorption capacities etc.).

The ExpaAsym cellular core was designed to account for this significant disadvantage of the honeycomb. Its relative density has been reduced by approximately half in comparison to the honeycomb with values in the range $[0.06-0.018]$. In the case where the expansion angle is equal to

60°, the result is a honeycomb-like structure, which provides the advantages such as reducing the material usage by 50%, while providing a consistent adhesion surface as opposed to its correspondent. In addition to these two benefits, it is also significantly easier to manufacture, and thus it represents a potentially less expensive solution.

For the newly developed cellular structure, the relative density is comparable with the one of the ExpaAsym and varies in the range of [0.06-0.025]. Having a similar manufacturing process, the main advantage the pyramidal topology provides is the enhanced bonding surface, which is significantly enlarged compared to ExpaAsym.

The pyramidal cellular core has been developed to keep up with the demands on the nowadays market. The main advantages offered by this new design are: *i*) a low relative density of the core and *ii*) a significant bonding surface. Together with a simple manufacturing process, they represent an important set of assets in the attempt in making a difference in the design of lightweight structures.

3.5 Conclusions

The parametric study performed on the novel pyramidal core has shown that for all the geometric configurations taken into consideration, the bulk dimensions of the cell unit with respect to the inclination angle of the struts has the same behaviour. In this regard, the following conclusions can be drawn:

- The length of the cell unit is indirectly proportional to the inclination angle; its value drops together with the increase in value of the angle.
- The width and height of the unit cell is directly proportional to the angle of expansion of the corrugation.
- The minimum value of the relative density was registered in the range of [30°-70°] for all the nine configurations subjected to study.
- The values for the relative density drop together with an increase of the radius of the perforation, R .

To validate the influence of the radius of the perforation, R , on the behaviour of the pyramidal structure, it is imperative to define its mechanical properties. In this regard, the strength and stiffness of the unit cell have been furtherly investigated through analytical and experimental means and the correlation between the two models was performed. This study is presented in the following chapter.

4. Theoretical and experimental analysis of the novel pyramidal cellular structure

4.1 Out-of-plane compression properties of the unit cell

The out-of-plane stiffness and strength of the pyramidal cellular structure under study is estimated by building an analytical model. An experimental model is also designed and experimental tests are conducted to validate the theoretical approach. The properties of the novel cellular structure are evaluated through a comparative study with other existing configurations to evaluate its potential into the market.

4.1.1 Analytical modelling

Due to the symmetry of the pyramidal structure, a quarter of the unit cell has been identified and considered for developing the analytical model. This consists of two segments, which represent the free members of the system subjected to external loading, Figure 4.1 [73].

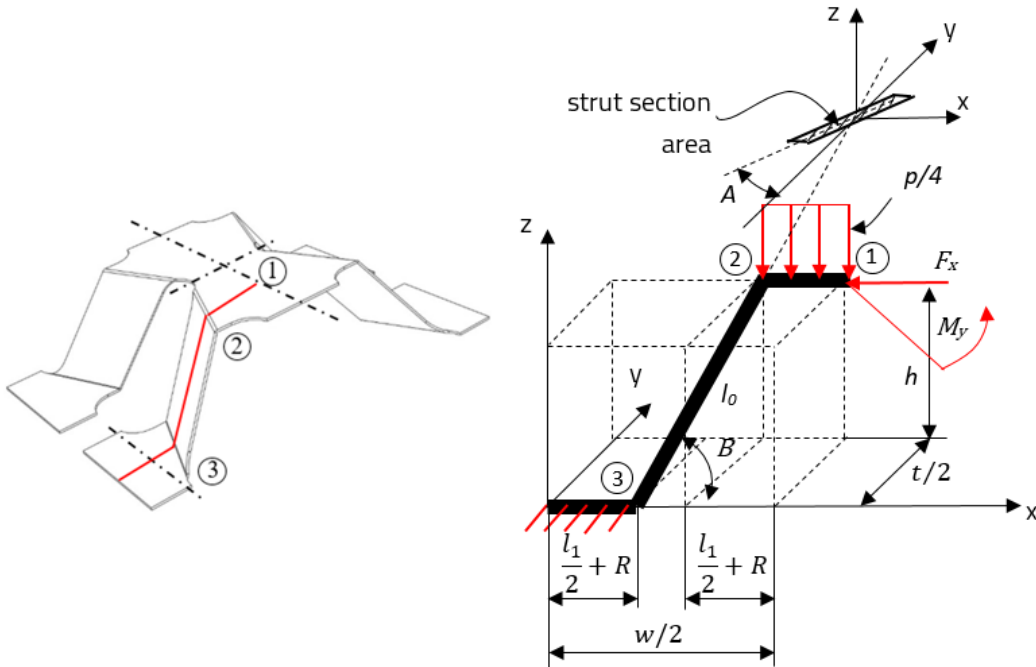


Figure 4.1 Quarter of unit cell under out-of-plane compression loading [73].

The load the system is subjected to is represented by a uniformly distributed pressure, p , acting on segment 1-2. This pressure is applied in the global coordinate system, in the z direction and generates a vertical displacement, δ_z . The boundary conditions of the system consist in setting to zero all DOFs in point 3.

This equivalent model formulation was successfully applied to several types of corrugations [81, 82, 83, 84] and to expanded hexagonal structures [36].

The equations defining the bending moments and tangential forces acting on each constituent element, in an arbitrary point x of the system are:

$$M_{1-2} = \frac{-F_z}{4}x - \frac{p}{4}x\frac{x}{2} + M_y \quad (4.1)$$

$$M_{2-3} = \frac{-F_z}{4}\left(\frac{l_1}{2} + R + x\cos(B)\right) - \frac{p}{4}\left(\frac{l_1}{2} + R\right)\left(\frac{l_1}{2} + R + x\cos(B)\right) + F_x\cos(A)x\sin(B) + M_y \quad (4.2)$$

$$T_{1-2} = \frac{-F_z}{4} - \frac{p}{4} \quad (4.3)$$

$$T_{2-3} = \frac{-F_z}{4}\cos(B) - \frac{p}{4}\cos(B) - F_x\sin(B)\cos(A) \quad (4.4)$$

Applying Castigliano's second theorem [80], which states that, for deformations in the linear elastic regime, the vertical displacement, δ_z , the rotation in point 1, $\delta_{\theta_{M_0}}$ and its horizontal displacement, δ_x can be computed as follows [74]:

$$\delta_z = p \left(\frac{\frac{2R + l_1}{32Gcg} - \frac{12l_0^2 \left(\frac{\cos(B)(R + \frac{l_1}{2})(\frac{R}{2} + \frac{l_1}{4})}{32} + \frac{\cos(B)(R + \frac{l_1}{2})(\frac{R}{4} + \frac{l_1}{8})}{8} \right)}{Eg^3(2R - c)} + \frac{l_0^3 \cos(B)^2 (R + \frac{l_1}{2})}{4} + 3l_0(R + \frac{l_1}{2})(\frac{R}{2} + \frac{l_1}{4})(\frac{R}{4} + \frac{l_1}{8})}{Eg^3(2R - c)} \right) \\ + \frac{12l_0^2 \left(\frac{M_y \cos(B)}{8} + \frac{F_x \cos(A) \sin(B) (\frac{R}{4} + \frac{l_1}{8})}{2} + 12l_0 M_y (\frac{R}{4} + \frac{l_1}{8}) + F_x l_0^3 \cos(A) \cos(B) \sin(B) \right)}{Eg^3(2R - c)} - \frac{3M_y (R + \frac{l_1}{2})^2}{2Ecg^3} \\ - \frac{F_x l_0 \cos(A) \cos(B) \sin(B)}{4Gg(2R - c)} \quad (4.5)$$

where:

$$M_y = \frac{p2E(6R^2g^2(cl_1 + 2cl_0 - l_1^2) + 4R^3g^2(c - 3l_1) + Rg^2(12\cos(B)l_0^2c - 12cl_0l_1 - l_1^3 + 6cl_1^2) - 8R^4g^2)}{96(ERg^2(2c - 4Rl_1 + 2cl_0 + cl_1) + Gl_0(2cl_0^216R^2l_0 + 8Rcl_0 - 8Rl_0l_1 + 4cl_0l_1))} \\ + \frac{pG(8Rl_0l_1(3cl_0^2 - l_0l_1^2 + 3cl_0l_1) - 64R^2l_0^2 + 24R^2l_0(cl_0^2 + 2l_0l_1^22cl_0l_1) + cl_0l_1(4l_0l_1 + 6l_0^2l_1))}{96(ERg^2(2c - 4Rl_1 + 2cl_0 + cl_1) + 2Gl_0^2(cl_016R^2 + 4Rc - 4Rl_1 + 2cl_1))}$$

$$F_x = \frac{p2Eg^2 \cos(B) (2R(2R - c + l_1) - (2cl_0 - cl_1))}{8 \cos(A) \sin(B) ((Eg^2(2Rc - 4R^2 - 2Rl_1 + 2cl_0 + cl_1)) + 2G(cl_0^3 - 8R^2l_0^2 + 4Rcl_0^2 - 4Rl_0^2l_1 + 2cl_0^2l_1))} \\ + \frac{pG(-16R^4l_0 - 8R^3l_0(3l_1 + c + 4l_0 \cos(B)) - 4R^2l_0(8\cos(B)l_0l_1 - 4\cos(B)l_0c + 3l_1^2 - 3cl_1) - 2Rl_0(2\cos(B)cl_0^2 - 4\cos(B)l_0l_1^2 + 8\cos(B)cl_0l_1 - 3l_1^2 + 3cl_1^2))}{8 \cos(A) \sin(B) ((Eg^2(2Rc - 4R^2 - 2Rl_1 + 2cl_0 + cl_1)) + 2G(cl_0^3 - 8R^2l_0^2 + 4Rcl_0^2 - 4Rl_0^2l_1 + 2cl_0^2l_1))} \quad (4.6)$$

The effective strain in the system is defined as:

$$\varepsilon_z = \frac{\delta_z}{h} \quad (4.6)$$

where h is the height of the unit cell, with w and t are the length and the width of the unit cell (detailed in chapter 3).

The effective stress acting on the structure is computed using equation (4.7)

$$\sigma_z = \frac{pl_1}{A_s} \quad (4.7)$$

where $A_s = wt/4$ is the compressive area of the structure, with w and t are the length and the width of the unit cell (detailed in chapter 3)

The effective stiffness of the structure is further calculated using equation (4.8):

$$E_z = \frac{\sigma_z}{\varepsilon_z} \quad (4.8)$$

By substituting equation **Error! Reference source not found.**, and equation **Error! Reference source not found.** into equation **Error! Reference source not found.**, the expression for the out-of-plane compressive stiffness of the structure is obtained.

The assessment of the out-of-plane compressive strength of the pyramidal corrugation is performed by assuming the failure mode of the struts identical to Euler's buckling. This states that a slender column subjected to longitudinal compressive load will fail due to sudden bend or buckling. The critical load in this case can be computed using the following equation [85]:

$$F_{cr} = \frac{\pi^2 EI_{2-3}}{4(0.6l_0)^2} \quad (4.9)$$

where I_{2-3} is the moment of inertia for the cross-section of the strut.

Applying the beam theory on the given system, an effective length factor of 0.6 was used. The approximation was determined as an average value between the fixed-fixed condition (0.5) and the fixed-pinned condition (0.7) considering the influence of the radius of the perforation R , has at the end of the struts.

The out-of-plane compressive strength can be evaluated using the following equation:

$$\sigma_z = \frac{F_z}{A_s} \quad (4.10)$$

where $F_z = \frac{F_{cr}2\cos(A)}{\sin(B)}$ and $A_s = wt/4$.

Finally, equation (4.19) becomes as follows, and defines the out-of-plane strength of the pyramidal structure [74]:

$$\sigma_z = \frac{2 \frac{\pi^2 EI_{2-3} \cos(A)}{(0.6l_0)^2}}{wt \sin(B)} \quad (4.11)$$

4.1.2 Numerical investigation of the buckling modes of the cellular structure

The numerical model for the out-of-plane compression analysis of the unit cell is presented in Figure 4.2. The specimen (marked 1), previously glued to the steel support plate (marked 2) is subjected to a compression loading scenario between the support block (marked 3) and the load block (marked 4).

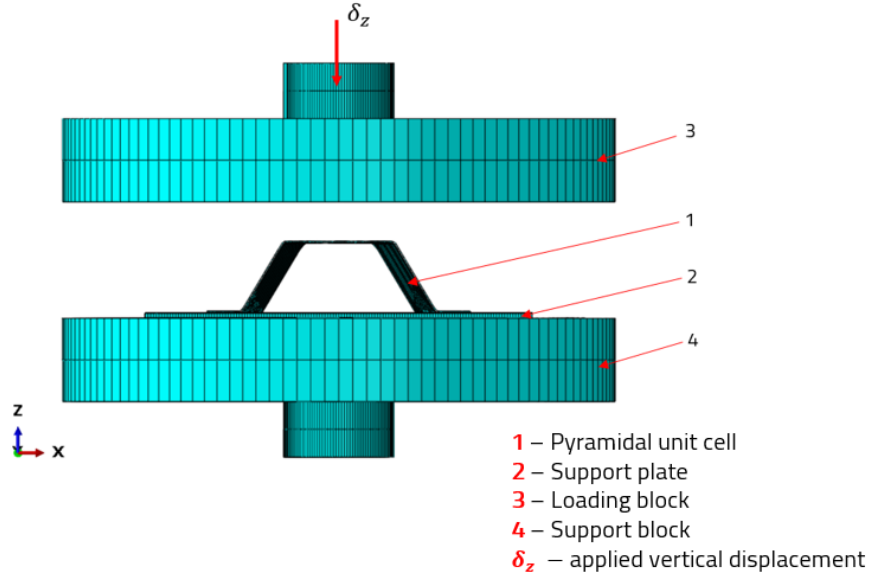


Figure 4.2 Out-of-plane compression setup for the numerical model.

4.1.3 Experimental approach

The experimental investigation aims to validate the analytical model defined for computing the strength and stiffness of the pyramidal cellular structure as well as the buckling modes of the unit cell's strut computed with the help of the numerical model.

■ *Sample preparation*

The samples for the pyramidal structure were created from a stainless-steel type 304 ($E = 187000 \text{ MPa}$) sheet metal with a thickness of 0.25 mm.

The perforations were made on a water jet cutting machine Maxiem 1530, Figure 4., equipped with a 20 HP hydraulic pump, which can sustain a constant water pressure of 3500 bar [73].

■ *Investigated geometric configurations*

The studied geometric configurations of the pyramidal cellular structure were obtained by using a set of fixed parameters $B = 60^\circ$, $l_1 = 10\text{mm}$, $l_0 = 15\text{mm}$ and $c = 15\text{mm}$, and a variable parameter $R = [3, 4, 5] \text{ mm}$. This resulted in three configurations named C1 ÷ C3, shown in Table 4.1.

Table 4.1 Configurations and dimensions of the samples for the compression tests [73].

Configuration	w [mm]	t [mm]	h [mm]	B [°]	A [°]
C1	47	37	13.3	60	21.8
C2	51	38	13.3	60	28.1
C3	54	39	13.3	60	33.7

The expanded unit cells were glued to individual 1 mm thickness steel plates to fix the movement of the struts during the tests.

To ensure repetition of the structural behaviour, three samples for each configuration have been considered. The compression tests were performed on an **Intron 3360 testing unit**. They were displacement controlled with a constant crosshead speed of 3 mm/min and the load was measured using a 5kN load cell. The compressive stress was computed by dividing the measured load by the surface area of the unit cell ($w \times t \text{ mm}^2$). The compressive strain was calculated by dividing the crosshead displacement by the initial height of the core.

The out-of-plane elastic modulus was determined on the slope of the experimental stress-strain curve as $E_z = \sigma_z / \varepsilon_z$.

4.2 Validation of the theoretical model

The out-of-plane compression tests have provided values for the strength (σ_z) and effective elastic modulus (E_z) for a single unit cell with the strut inclination angle equal to 60°. The comparison between the experimental and analytical results is presented in Table 4.2.

Table 4.2 Analytical and experimental results for the out-of-plane compression [73].

Configuration	Analytic		Experimental	
	E_z [MPa]	σ_z [MPa]	E_z [MPa]	σ_z [MPa]
C1	15.4	0.33	15.15	0.286
C2	9.08	0.22	9.04	0.196
C3	5.43	0.13	5.05	0.12

The measured experimental values for the maximum strength and stiffness are slightly lower than the theoretical ones. This is due to the fact that the analytical model does not include the geometric imperfections of the unit cell's struts obtained during the expansion process.

In addition, the value for the guiding radii is approximated to zero in the analytical model, while, for the experimental testing, the value for the bends' radii is approximatively 1 mm. The role of the bend radius

is critical; it contributes to avoiding the crack propagation in the sheet metal during the expansion process.

The comparative study between the two models shows that both, the analytical and the experimental ones, follow the same path. This outlines that the analytical model was successfully validated through experimental testing.

The buckling modes of the unit cell's struts were identified with the help of the numerical model subjected to similar boundary conditions and loading scenario as the experimental setup, Figure 4.3.

A comparison between the observed deformations and FE predictions of the quasi-static buckling modes for all the configurations subjected to experimental testing was performed.

The FE prediction shows the same buckling shape for all of the cell's struts, located approximately in the middle region of the structure.

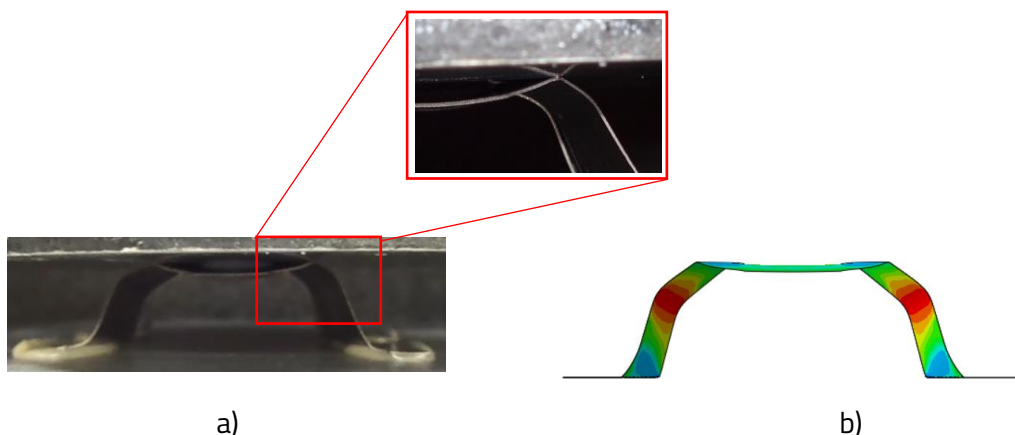


Figure 4.3 A comparison between the observed and FE predictions of the deformation mode for configuration C1 (a) observed shape (b) FE prediction.

The results for configuration C2 shows the same behaviour as for the C1 configuration; the four struts of the unit cell registered an outwards buckling shape on the medial transversal axis.

The comparison between the two models for the C3 configuration are in good agreement.

The comparison between the numerical and experimental models suggests that the FE predictions are effective in illustrating the buckling shapes of the struts as they occur in reality, thus confirming the possible use of the validated numerical model for future investigations. Despite this, further investigations should consist in analysing how does the value of the bend radii influence the deformation pattern of the struts and what is the influence on the overall mechanical properties.

Based on the validated analytical model, the out-of-plane mechanical properties of the pyramidal structure can be evaluated by varying the defining geometric parameters of the unit cell.

Figure 4.4 shows the evolution of the specific compressive stiffness and strength, E_z/ρ and σ_z/ρ , for the investigated structure.

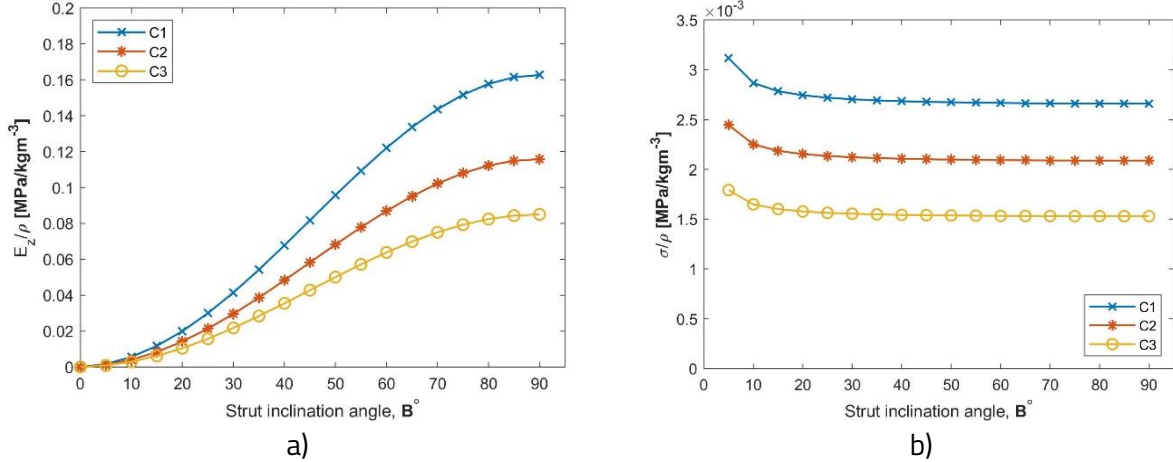


Figure 4.4 Compressive properties of the investigated structure: a) compressive stiffness; b) compressive strength [73].

The variable parameter for this study is the strut's inclination angle, $B = [0^\circ - 90^\circ]$, since this is one of the most important feature defining the topology of the corrugation. The constant parameters of the structure are $l_0 = 15\text{ mm}$, $c = 15\text{ mm}$, $l_1 = 10\text{ mm}$. The radius of the perforation is also variable and different for each configuration subjected to experimental investigations; $R = 3\text{ mm}$ for C1, $R = 4\text{ mm}$ for C2 and $R = 5\text{ mm}$ for C3.

First, as expected, the value of the stiffness of the pyramidal structure is directly proportional to the increase of the strut inclination angle B , Figure 4.10 a). Secondly, the specific stiffness decreases together with the increase of the perforation radius R which translates into an increase of the strut's slenderness.

This slenderness of the unit cell's strut is critical for the compressive strength of the structure, Figure 4.10 b). This decreases together with an increase of the perforation radius, R , which translates into an increase of the internal angle of the structure, A . This is because the strut of the cell is the main load bearing element. The highest values are recorded by the C1 configuration, where the radius of the perforation has the lowest value, $R = 3\text{ mm}$ [73].

4.3 Trapezoidal cellular structure

The studied geometric configurations of the trapezoidal cellular structure were obtained by using a set of fixed parameters $l_1 = 10\text{ mm}$ and $c = 15\text{ mm}$, $A = 0^\circ$ and a set of variable parameters, $R = [3, 4, 5]\text{ mm}$ and $l_t = [21, 23, 25]\text{ mm}$.

The values of the expansion angle B_t , were computed according to the following relation, $h = h_t$. This condition was imposed to ensure that both structures subjected to investigation, trapezoidal and pyramidal, remain of the same height. Comparing the projected area of the two unit cells, $A_{C_1} = 1739\text{ mm}$ and $A_{C_{1t}} = 1642\text{ mm}$, represents an efficient method to highlight the advantages of the

internal angle of the pyramidal structure, A . The value of the expansion angle was defined as, $B = [38.24^\circ, 35.32^\circ, 32.14^\circ]$. This resulted in three configurations named C1t ÷ C3t, shown in Table 4.3.

Table 4.3 Configurations and dimensions of the trapezoidal samples for the compression tests.

Configuration	w_t [mm]	t_t [mm]	h_t [mm]	B_t [$^\circ$]	A_t [$^\circ$]
C1t	52.98	31	13.3	38.24	0
C2t	57.53	31	13.3	35.32	0
C3t	60.79	31	13.3	38.24	0

The trapezoidal samples were prepared and tested in the same conditions as the pyramidal structure as defined in Section 4.1.3. To ensure repetition of the structural behaviour, three samples for each configuration have been considered. The compression tests were performed on an **Intron 3360 testing unit** and were displacement driven with a constant crosshead speed of 3 mm/min. The load was measured using a 5kN load cell. The compressive stress was computed by dividing the measured load by the surface area of the unit cell ($w \times t$ mm 2). The compressive strain was calculated by dividing the crosshead displacement by the initial height of the core.

The out-of-plane elastic modulus was determined on the slope of the experimental stress-strain curve as $E_z = \sigma_z / \varepsilon_z$.

The comparison between the experimental and analytical results is presented in Table 4.4.

Table 4.4 Analytical and experimental results for the out of plane compression

Configuration	Analytic		Experimental	
	E_z [MPa]	σ_z [MPa]	E_z [MPa]	σ_z [MPa]
C1t	14.09	0.26	13.94	0.233
C2t	8.57	0.17	7.41	0.141
C3t	5.2	0.1	4.25	0.082

Similar to the behaviour of the pyramidal structure, the values for the maximum strength and stiffness measured by experimental means are slightly lower than the theoretical ones. This is due to the fact that the analytical model does not include the geometric imperfections of the unit cell's struts.

In addition, the value for the bend radii is approximated to zero in the analytical model, while, in the case of the experimental testing, their value is approximatively 1 mm.

Regarding the trapezoidal cellular structure, the comparative study shows that both, the analytical and the experimental models, follow the same path. This outlines that the analytical model developed for the pyramidal structure is also valid for the trapezoidal core.

The comparison between the out-of-plane performance of the trapezoidal and the pyramidal structures are shown in Table 4.5.

Table 4.5 Comparison between the out-of-plane properties of the pyramidal and trapezoidal cores

Configuration	C1	C1t	C2	C2t	C3	C3t
E_z [MPa]	15.4	14.09	9.08	8.57	5.43	5.2
Difference	9.29 %		5.95 %		4.42 %	
σ_z [MPa]	0.33	0.26	0.22	0.17	0.13	0.1
Difference	26.92 %		29.41 %		30 %	

The comparative study between the two topologies, pyramidal and trapezoidal shows that the internal angle, A , significantly increases the mechanical properties of the structure with an average of 6.5% in stiffness and 28.7 % in strength.

Another aspect worth investigating is the mechanical performance of the structure when the value of the internal angle of the structure, A , is independent from the radius of the perforation.

4.4 The variation of the internal angle

With respect to the values of the defining parameters, the variation of the unit cell's stiffness and strength, with respect to the internal angle of the structure, A , are depicted in Figure 4.5.

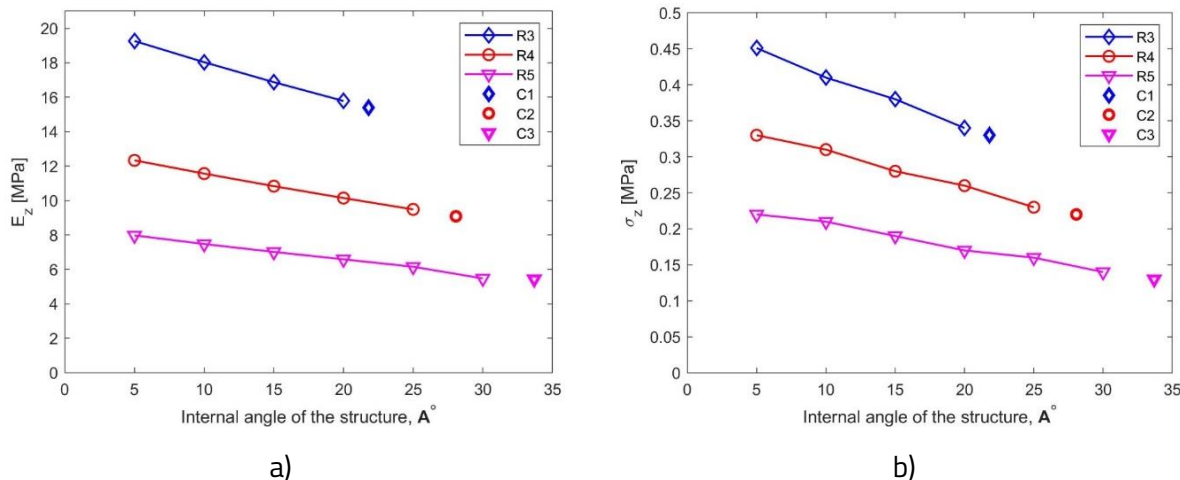


Figure 4.5 Variation of the mechanical performances with respect to the internal angle: a) compressive stiffness; b) compressive strength.

The value of the out-of-plane compression stiffness of the pyramidal structure is directly proportional to the decrease of the internal angle of the structure A ; the compressive properties of the trapezoidal structure decrease together with the increase of value of angle A .

4.5 Comparative study

After the out-of-plane stiffness of the structure under study has been defined and validated, the structural performance of the pyramidal cellular core has been compared with a selection of different core types used in the construction of sandwich panels, as shown in Figure 4.6.

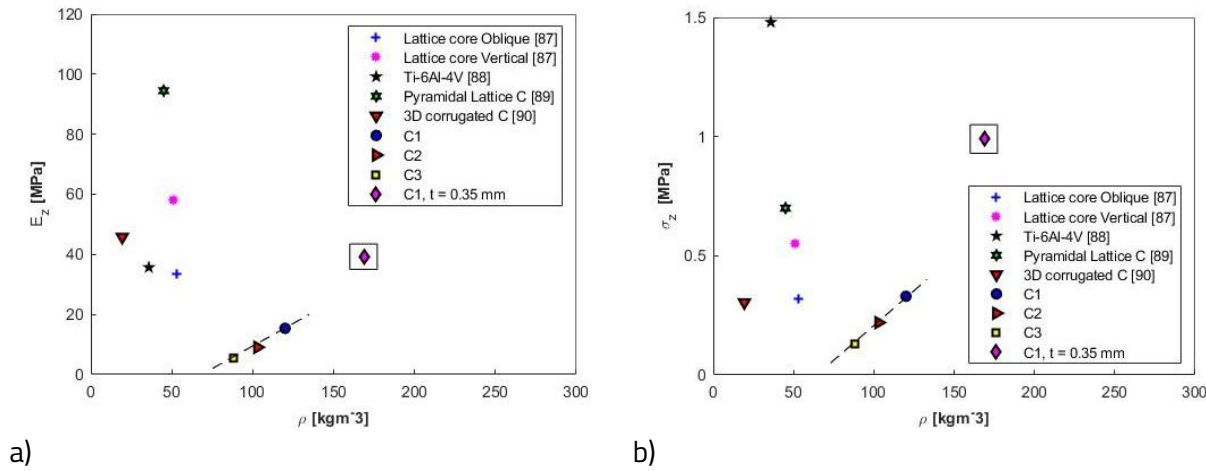


Figure 4.6 Effective compression properties several types of cellular structures: a) compressive stiffness; b) compressive strength [69].

The pyramidal structure exhibits lower compressive stiffness performance when compared to the other structures taken into consideration within the study, Figure 4.6 a). Despite this, it is imperative to mention that the thickness of the parent material of 0.25 mm is significantly reduced in comparison to the ones of the other studied structures (e.g. 0.9 mm for the carbon fibre/epoxy lattice core oblique and lattice core vertical developed by J. Xiong et. al [87] and 0.635 for the titanium alloy structure presented by Queheillalt and Wadley [88]). A decreased thickness of the base material makes the struts of the pyramidal structure under study more susceptible to buckling. However, by increasing the material thickness and considering $g = 0.35$, the stiffness of the structure, computed with the help of equation (4.16), becomes 42.36 MPa for a density of 175 kgm⁻³ and is marked in the rectangle on the graph. Through this modification, the novel structure exceeds the performances of the *Lattice core oblique* and the pyramidal corrugation obtained from an ultralight titanium alloy, *Ti-6Al-4V*. Compared to the *Pyramidal lattice C* developed by Ming Li et. al [89], the studied structure reaches half the stiffness value with a significant increase in density.

The out-of-plane strength with respect to core density is illustrated in Figure 4.6 b). The highest performance has been registered for the C1 configuration with a maximum stress of 0.33 MPa. With this value, the newly developed structure ranks above the *Lattice core oblique* corrugation with a

measured value of 0.32 and the 3D corrugated C presented by Jian Xiong et. al [87] but at a higher density. Increasing the base material thickness for the C1 configuration from 0.25 mm to 0.35 mm brings the investigated structure to a compression strength of 0.92 MPa which corresponds to a density of 175 kgm^{-3} .

The internal angle, A , was considered as function of the radius, R . This initial assumption turned into a limitation with respect to the performance of the structure (both stiffness and strength) due to the fact that increasing the angle A , the value of R needs to be increased as well, which results in a slender strut. Further investigations should consider a different formulation for the angle A , independent from the perforation radius R .

4.6 Conclusions

The main purpose of this chapter is to assess the structural performance of the novel pyramidal cellular in order to evaluate its potential use for the construction of sandwich panels. An analytical model was developed to define the out-of-plane compressive properties. The expressions defined for computing the maximum strength and stiffness were validated through experimental testing.

A finite element model was developed to predict the buckling shapes of the struts of the unit cell. The results were compared to the deformations observed during the performing of the experiments and have proven to be in good agreement.

The following conclusions can be drawn regarding the out-of-plane compressive performance of the pyramidal cellular structure under study:

- The out-of-plane elastic modulus, E_z , decreases together with the increase of the internal angle A . Since the latter is defined as a function of the radius of the perforation, R , this translates into an increase in slenderness of the unit cell's strut which makes the structure more susceptible to buckling. The compressive stiffness increases together with the increase of the inclination angle of the strut, B .
- The strength performance is decreased with the increase of the internal angle A . In addition to this, the effective compression strength of the structure is also decreasing together with an increase of the inclination angle of the strut, B .
- The proposed manufacturing process is expected to reduce material waste and production costs by providing a simple yet efficient manufacturing method. It provides a considerable degree of versatility by having the advantage of being manufactured from any ductile metal which can be formed into thin sheets.
- An increased overall structural performance (both stiffness and strength) is reached by considering the angle A independent from the perforation radius R .
- The stiffness and strength behaviour could be improved by increasing the second moment of inertia of the struts, for example, through embossing operations or by using low density materials.

5. Theoretical and experimental analysis of the sandwich panel with metallic pyramidal core

The performance of the sandwich panel based on the novel pyramidal cellular core is furtherly investigated in this chapter. The effective bending and shear stiffness and the deflection at midspan of the sandwich structure were determined by numerical and experimental approaches. The two models were found to be in good agreement. In this regard, the validated numerical model can be subsequently used for further product development. This may lead to providing better mechanical properties and higher lightweight capabilities.

5.1 Investigation of the bending stiffness

5.1.1 Numerical modelling

To evaluate the bending and shear stiffness of the sandwich beam, a four-point bending set-up has been considered, Figure 5.1. When a beam is subjected to four-point bending shear force, P , acting in the entire region between the outer and inner supports and the bending moment in the midspan are constant. This decreases the possibility of local failure due to buckling of the face sheets and provides a broader understanding of behaviour and mechanical properties of the core [3, 4].

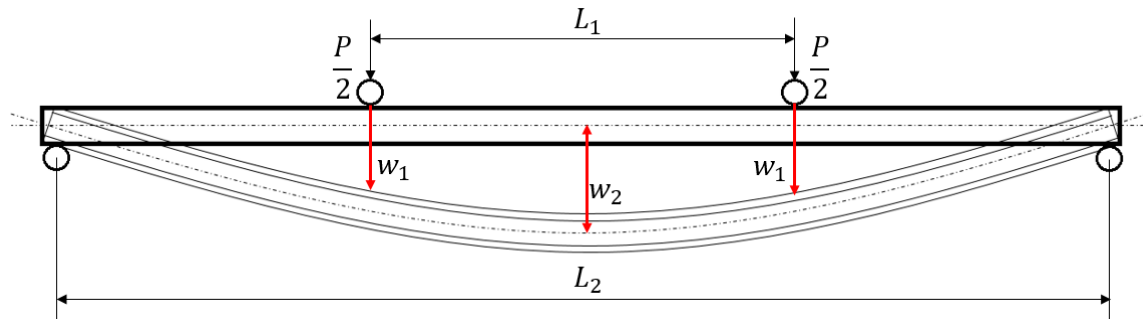


Figure 5.1 Schematic representation of the four-point bending setup [74].

The four-point bending setup helps in determining the relation between the imposed displacement w_1 , the resulting deflection, w_2 and provides values for the load, P . With respect to these parameters, the specific bending and shear stiffness can be computed with respect to the total mass of the beam, by using equations (5.6) and (5.7) [5, 1]:

$$D = \frac{PL_1^2(L_2 - L_1)}{m16w_2} \quad (5.1)$$

$$S = \frac{12DP(L_2 - L_1)}{m(12w_1DL_2 - P(L_1^3 - 3L_1^2L_2 + 2L_2^3))} \quad (5.2)$$

where: $m = (2\rho_{sk}t_f + \rho_r\rho_{sc}t_c)L_2b$ – total mass of the sandwich beam

with: $t_c - \rho_{sk,c}$ – the base material density for the face sheets and core respectively, t_f – thickness of the face sheets, ρ_r – relative density of the cellular core, thickness of the core, L_2 – active length of the sandwich beam, b – width of the sandwich beam.

To evaluate the four-point bending performance of the sandwich beam, the finite element model, depicted in Figure 5.2, was designed. The sandwich beam, which consists in two lateral faces (marked 3 and 5) applied on the two sides of the cellular core (marked 4) is subjected to a four-point bending loading scenario between support rollers (marked 6 and 7) and the loading rollers (marked 1 and 2).

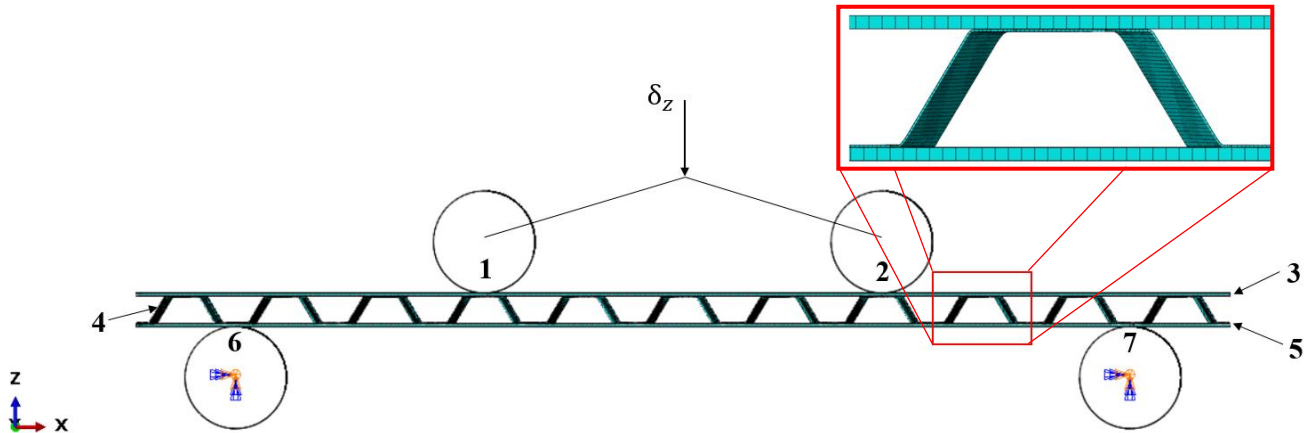


Figure 5.2 Four-point bending setup of the numerical model [74].

The components of the system are modelled using 4-node structural shell elements, S4R, a reduced integration element with 6 DOFs for each node, 3 translations and 3 rotations.

Components representing the rollers, marked 1, 2, 6 and 7 are modelled as analytical rigid bodies. The boundary conditions for the model are defined by restricting all DOFs for the support rollers, while an imposed displacement was applied for the loading rollers, perpendicular to the face sheets. The deflection at midspan is measured at a node on the top sandwich face sheet in the symmetry plane and the corresponding reaction force is registered at the bottom cylinders. The contact areas between the sandwich components (core and face sheets) are modelled as a node-to-surface contact and considered perfectly bonded. The contacts between the support and loading rollers and the sandwich face sheets is modelled as a surface-to-surface contact with a frictional coefficient of 0.17 corresponding to steel-to-steel interaction.

5.1.2 Analysis on the geometric imperfections

When defining the bending and shear stiffness of sandwich panels with periodic cellular cores by using numerical models, simulation results are usually higher than experimental values especially in the out-of-plane direction. This occurs due to the imperfections in the cellular structure generated by undesired variations of the geometric parameters during the manufacturing process [2].

Accounting the geometric imperfections implies the superposition of buckling eigenmodes onto the initial geometry before applying the load. The first step consists in performing a linear buckling analysis to compute the most probable collapse modes. The evaluation of the buckling shapes enables the choice of the modes which might generate the most critical imperfections (the lowest buckling modes are assumed to provide the best approximation). The buckling eigenmodes are subsequently written according to the global coordinate system as nodal displacement [91].

From the computed buckling shapes mode 1 was considered to have the highest probability in generating critical initial deformation. The distorted nodal coordinates are applied with scaling factor of 0.1. This perturbation generated on the initial core geometry allows the nodes to translate in the direction set by the eigenmode by 10% of the value of the initial displacement U_i .

5.1.3 Experimental approach

The experimental investigation was aimed to validate the numerical model for computing the bending and shear stiffness of the sandwich beams based on the pyramidal cellular core. To ensure the reproducibility of the bending behaviour, three samples for each configuration were considered during the experimental testing.

■ *Manufacturing of specimens*

The cellular core was manufactured from stainless-steel type 304 with a thickness of 0.25 mm.

The face sheets had a thickness of 1.5 mm and were obtained from mild carbon steel with the elastic properties listed in section 5.1. The cellular core was bonded to the face sheets using Araldite 2015®, an epoxy based bi-component adhesive produced by Huntsman. The adhesive is applied using a manual glue gun with a mixing nozzle to keep the mixing percentage as recommended by the manufacturer, Figure 5.3 a). The sandwich assembly is depicted in Figure 5.3 b).

The position of the sandwich beams during the experimental procedure, for all the configurations considered for the study, is shown in Figure 5.3 c).

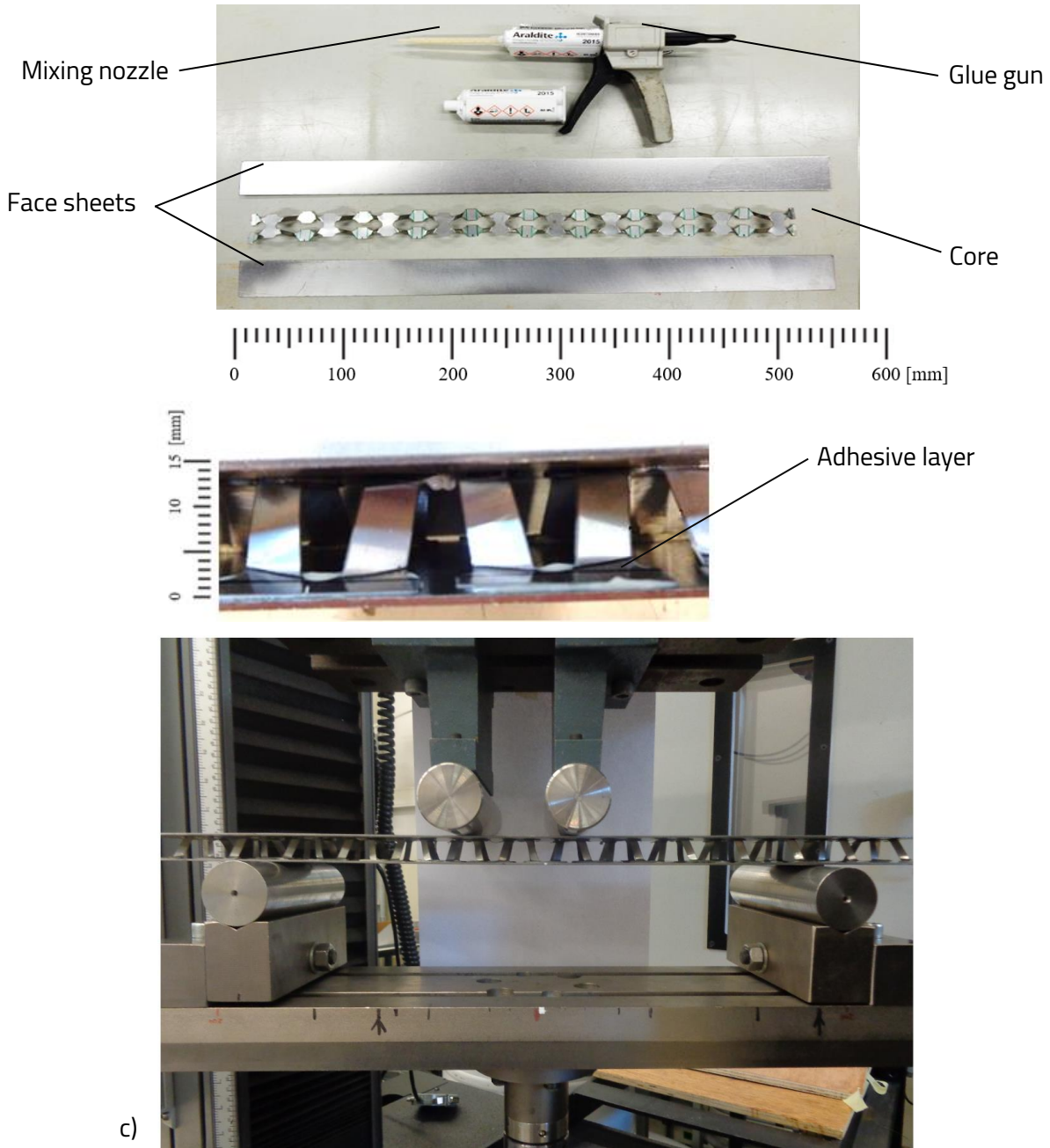


Figure 5.3 a) Component elements of the sandwich assembly; b) assembled sandwich structure; c) position of the sandwich beam in the testing unit [74]

■ *Investigation of geometric configurations*

The geometric configurations for the cellular core were obtained by considering several parameters to be constant, $B = 60^\circ$, $l_1 = 10$ mm, $l_0 = 15$ mm and $c = 15$ mm and the radius of the perforations variable $R = [3, 4, 5]$ mm, which results in a variation of the expansion angle A . Both expansion directions of the cellular core, x and y , were considered when manufacturing the samples. This resulted in obtaining six configurations named C1X ÷ C3X and C1Y ÷ C3Y respectively, Table 5.1.

Table 5.1 Experimental configurations and dimensions of the samples for the four-point bending tests [74].

Configuration	Beam length [mm]	Beam width [mm]	Beam height [mm]	Internal angle, A [°]	Loading span, L ₁ [mm]	Support span, L ₂ [mm]
C1X	533	37.9	18.09	21.8	183	419
C1Y	525	45.09	18.15	21.8	180	416
C2X	550	37.77	18.56	28.1	95	343
C2Y	535	50.94	18.82	28.1	104	364
C3X	568	38.28	19.12	33.7	61	366
C3Y	550	54.86	19.49	33.7	73	381

The dimensions for the shear- and mid- spans were chosen by considering the specimen's topology , thus the loading rollers sheets correspond to the middle of the glued area between the unit cell's top surface and the face sheets.

■ *Experimental protocol*

The four-point bending tests were performed on an Instron 2985 testing unit, they were displacement driven and the cross-head speed was kept constant at 1 mm/min. An imposed displacement of 3 mm was applied and the load was measured using a 30kN load cell.

The deflection at midspan, w_2 , was registered using Digital Image Correlation (DIC) throughout the experimental procedure. The use of the system ensures the correlation between the analogue data (e.g. displacement, registered load) for each registered image.

The maximum deflection at midspan, w_2 , was determined on the slope of the load-displacement graph in the elastic region and can be defined as: $w_2 = h_1 - h_0$, Figure 5.4.

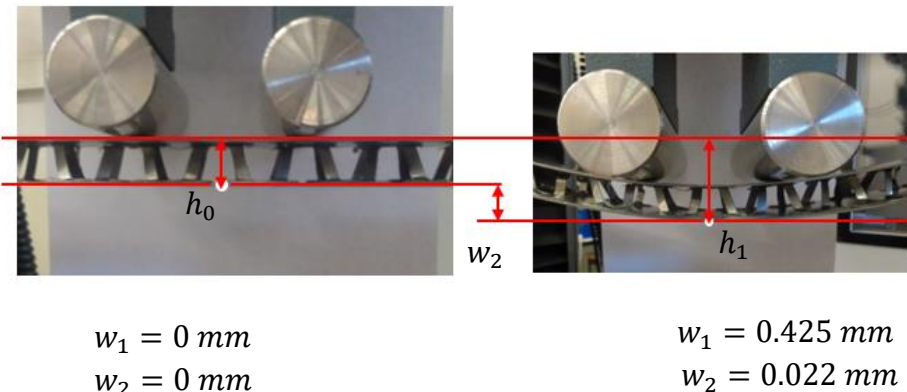


Figure 5.4 Method for extracting the value of w_2 : h_0 – the initial position of the sandwich beam; h_1 – the position of the beam corresponding to the given displacement for each configuration [74].

5.2 Validation of the numerical model – correlation between numerical and experimental results

The four-point bending tests have provided values for the load (P), displacement (w_1) and deflection at midspan (w_2) for each of the specimens subjected to the experimental procedure. The results are presented in Table 5.2 as comparison between the experimental and numerical results. The value for the displacement (w_1) is the same for both the numerical and experimental models, to ensure an accurate correlation for the effective bending properties, Table 5.2.

Table 5.2 Numerical and experimental results for the four-point bending loading [74].

Configuration	Experimental results			Numerical (FE) results	
	Load [N]	w_2 [mm]	w_1 [mm]	Load [N]	w_2 [mm]
C1X	70.31	0.022	0.425	81.45	0.021
C1Y	44.04	0.021	0.246	77.19	0.023
C2X	33.59	0.003	0.3	51.91	0.004
C2Y	42.12	0.0034	0.25	73.32	0.005
C3X	27.18	0.004	0.27	32.07	0.005
C3Y	24.12	0.0052	0.25	30.77	0.006

The experimental values registered for the maximum load are slightly lower than the ones obtained by numerical means. This was to be expected since the numerical model does not consider the thickness of the adhesive layer used to assemble the sandwich beam. The values for the beam height are slightly lower in the case of the numerical model as opposed to the samples subjected to testing. However, in the considered setup, this does not significantly influence the mechanical properties of the core.

In addition to this, the geometric imperfections of the sandwich face sheets are not taken into consideration for the numerical model. This influences the values for the deflection at midspan which are lower for the samples subjected to experimental testing as opposed to the numerical model.

Table 5.3 shows the comparison between the numerical values resulted from finite element simulation and the values measured during the experiments, for the bending and shear stiffness.

Table 5.3 Comparison between the numerical and experimental values for the investigated sandwich structures [74].

	D_m [kNm ² /kg]	S_m [kN/kg]
	3.0	0.221
C1X	4.63	0.227
	4.51	0.224
D_m – average	4.05	0.224
D_m – FEA	4.68	0.287
	1.49	0.151
C1Y	3.23	0.313
	1.28	0.129
D_m – average	2.01	0.198
D_m – FEA	3.47	0.341
	4.25	0.258
C2X	3.41	0.237
	6.04	0.301
D_m – average	4.57	0.266
D_m – FEA	6.29	0.326
	3.22	0.197
C2Y	4.03	0.271
	5.56	0.392
D_m – average	4.27	0.286
D_m – FEA	6.5	0.412
	1.27	0.236
C3X	1.38	0.245
	1.33	0.241
D_m – average	1.32	0.241
D_m – FEA	1.55	0.291
	0.83	0.141

C3Y	0.96	0.165
	0.81	0.126
D_m – average	0.87	0.144
D_m – FEA	1.13	0.189

By comparing the numerical and experimental results it can be concluded that the two models exhibit the same trend. Although deviations between the sets of physical and virtual experiments are observed for some configurations, it is considered that the phenomena which presented by both models are in good agreement.

Since the shear- and mid- spans were different for all the configurations, the structural performance of the sandwich beam can be highlighted with respect to the two expansion directions defined on the corrugation: ox and oy .

The mechanical properties of the sandwich beam depend on the expansion direction of the corrugation. The slenderness of the strut (determined by the value of the perforation radius, R) as well as the distance between the top and bottom adhesion surfaces (defined by the length and width of the unit cell of the core) also have a significant influence on the structural performance of the assembly.

Analyzing the values in Table 5.3 a difference between the experimental and FE curves is revealed. This can be justified by the fact that for some of the samples subjected to experimental testing, a premature failure in the adhesive layer occurred prior to core failure (e.g. sample 1 for the C2X configuration).

Due to the fact that the mechanical expansion process does not involve forming the core in a positive-negative die (e.g. cold forming in molds) geometric imperfections are likely to appear. If the interdependence between the geometric parameters are not respected accordingly, planarity deviations of two or more adjacent adhesion surfaces may occur. If a deviation in height between the four struts of one unit cell is registered, then the contact between the core and face sheets is not met., thus the load transfer between the components is inefficient. This, together with an uneven application of the adhesive layer might lead to premature failure. Specimen 1 for the C2X configuration, registered a premature adhesive failure for a displacement $w_1=0.23$ mm. This justifies the change in trend of the load-displacement curve of the tested sample.

Regarding the specific bending stiffness, susceptibility to failure was observed on the direction corresponding to the y axis as opposed to the x axis of the sandwich beam, for the C1 and C3 configurations. The difference registered is significantly higher for the C1 configuration with a value of 4.68 kNm²/kg for case C1X as opposed to 3.47 kNm²/kg for case C1Y.

The C3Y configuration recorded a decrease of the same magnitude, with a drop in value of approximately 25% in comparison to C3X.

However, a completely different behaviour was shown in the case of the C2 configuration. With respect to bending stiffness, the two configurations (C2X and C2Y) register the same value of $6.5 \text{ kNm}^2/\text{kg}$. This shows that the topologic configuration of the unit cell, defined by the geometric parameters, is more homogeneous and exhibits similar bending behaviour on both of the in-plane directions.

In terms of shear stiffness, the trend shows an opposite behaviour. The C1Y configuration registered an improvement of approximately 16% for the shear stiffness when compared to C1X. This is due to the fact that the expansion in the y direction results in a more compact and the inclined position of the struts provides better shear stability for the structure. A similar effect is observed for the C2X configuration with a value of 0.287 kN/kg in comparison to 0.341 kN/kg for C2Y.

Nonetheless, the C3 configuration did not exhibit the same behaviour. The shear stiffness for C3X is reduced by approximately 35 % as opposed to C3Y.

This proves that, together with the decrease of the perforation radius, which influences the slenderness of the strut, the beam becomes more susceptible to shear failure.

In addition to this, for the C3 configuration, a significant difference between the experimental and numerical values is encountered. This suggests that, together with an increase of the radius of the perforation ($R = 5 \text{ mm}$), the corrugation might become more susceptible to geometric imperfections through the strut's width during the mechanical deformation process. The mechanical properties of the structure are also decreasing together with an increase of the spans between adjacent adhesion surfaces.

5.3 Comparative study

Accounting the good agreement between the two designed models, numerical and experimental a comparative study between the structural performance of the sandwich beams based on the pyramidal core and other proposed solutions is performed. The comparative results, with respect to the bending and shear stiffness are depicted in Figure 5.5. The C2 configuration is considered the best candidate for further development due to the similarity in bending stiffness for C2X and C2Y. This could lead to further improvement of the mechanical properties. The possibility of a reduction in density is also considered [74].

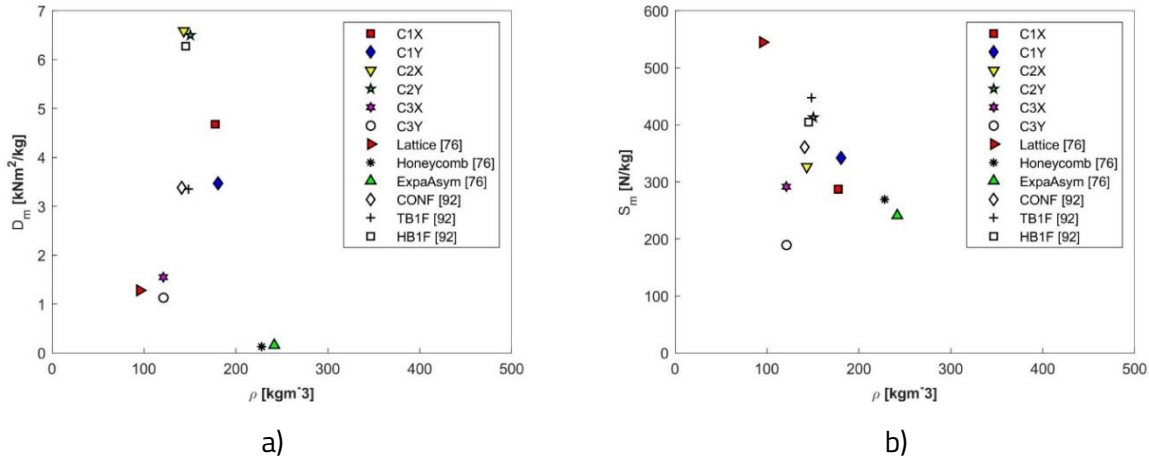


Figure 5.5 Specific bending stiffness as function of core density for the beams subjected to study [74].

The novel pyramidal core shows high potential for the construction of sandwich panels with a considerable improvement in bending stiffness and a significant reduction in density when compared to state-of-the-art honeycomb core. This was observed for all the configurations considered throughout the comparative study, Figure 5.5 a) [76, 92].

Configurations C2X and C2Y registered the highest bending stiffness with a value of $6.5 \text{ kNm}^2/\text{kg}$.

The lowest bending performance, with an effective stiffness of $1.15 \text{ kNm}^2/\text{kg}$, is registered for the C3Y case. Although it is ranked above some of the configurations proposed for the comparative study, it is still exceeded by the lattice-based assembly with improved mechanical properties and a density of 95.3 kg/m^3 . The C3X configuration presents a slightly improved bending stiffness but a higher value of the density.

The internal angle A , was proven to have a positive influence on the mechanical performance of the pyramidal structure since the novel core is ranked higher as the lattice structure which has a similar topology but with an internal angle equal to zero ($A = 0^\circ$).

Further optimization of the pyramidal core may lead to a reduced density while maintaining/ increasing its mechanical properties.

In terms of shear stiffness, Figure 5.5 b), the highest value was registered for the C2Y configuration with a value of 341.07 N/kg . This ranks the newly developed cellular core above most of the structures considered within the comparative study. Nonetheless, its shear performance is exceeded by the lattice corrugation [76], with a value of 0.545 kN/kg for a density of 95.36 kg/m^3 .

Regarding shear performance, configuration C3Y ranks lower than the ExpaAsym and the honeycomb, but at a significantly reduction density.

Further investigations may consist in improving the bending and shear performance by changing the core material from stainless steel to a one with a lower density (e.g. aluminium, titanium etc.) and the

face sheets from steel to carbon fibre reinforced composites. This is expected to translate into a significant decrease in density, which is a topic of interest for future investigations.

5.4 Conclusions

The main objective of this chapter was to assess the bending performance of a sandwich beam based on a metal-made pyramidal cellular core, obtained through a mechanical deformation process. The bending and shear stiffness were computed through finite element calculations and validated through physical experiments.

The following conclusions with respect to the proposed sandwich configurations can be written:

- The internal angle A is an effective method of increasing the mechanical performance of the pyramidal structure.
- To reach a maximum potential of the sandwich panel, the C2 geometric configuration was proven to be the best candidate for future investigations and optimizations, due to the high values registered for the bending stiffness and strength and to their similarity.
- The investigated pyramidal corrugation shows a high potential in competing with other concepts based different cellular topologies.
- The overall bending performances may be increased by replacing the material of the core and face sheets with a high-end low-density material (e.g. aluminium, carbon fibre reinforced composites etc.).

6. General conclusions and original contributions

This doctoral thesis addresses one of the main research problems related to the design of advanced lightweight cellular cores and to the construction of the associated sandwich panels, aimed at developing solutions for reducing material loss and overall production costs.

In this regard, a novel pyramidal cellular core was proposed for investigation. Obtained through a simplified manufacturing process, i.e. mechanical expansion, it offers the advantages of reducing material loss and provides a significant adhesion surface for a better contact between the core and the face sheets. This translates into providing a better structural stability for the associated sandwich panel.

The study of the mechanical properties aimed to contribute to a better understanding of the structural behaviour of the periodic cellular core, at the same time identifying new possibilities for further optimization and performance increase.

The scientific objectives initially formulated were successfully achieved by following the proposed research steps. The results provided by the research conducted in this regard have led to conclusions, as follows.

The critical review of the state of the art on advanced lightweight structures used in sandwich panel construction has shown that the demand for high-performance structures is still increasing nowadays. The raising awareness on the effect of the technological evolution on the environment leads to the necessity of implementing lightweight structures in all industrial fields – aerospace, naval, automotive, civil, and industrial construction, which is crucial for complying to the continuously emerging regulations.

Research conducted up to the present in this field has highlighted the following aspects:

- A multitude of existent materials can be considered (metallic or non-metallic).
- Newly developed cellular cores should provide performant topologies and offer a significant number of advantages: low density; high strength and stiffness both for in-plane and out-of-plane loading, high impact energy absorption, thermal and acoustic insulation.

The parametric study performed on the novel pyramidal corrugation has shown that the proposed manufacturing process provides a complex yet versatile structure with multifunctional potential.

The novelty feature of this corrugation, the internal angle A , is effective in designing a structure with an attractively low relative density.

The mechanical properties of the novel pyramidal cellular were evaluated by both analytical and experimental approach, to evaluate its potential use for the construction of sandwich panels. In this

respect, the out-of-plane compressive properties were analytically defined and validated through experimental testing. Thus, the analytical model can be furtherly used in conducting optimization processes to maximally exploit the performance of proposed structure.

The following conclusions can be drawn regarding the out of plane compressive performance of the pyramidal cellular structure under study:

- The out-of-plane elastic modulus, E_z , decreases together with the increase of the internal angle A . The compressive stiffness increases together with the increase of the inclination angle of the strut, B .
- An increase of the internal angle A and of the inclination angle of the strut, B , translate into a decrease in compressive strength.

The bending performance of the sandwich beam based on a novel pyramidal cellular core, was investigated by numerical modelling and experimental testing. The designed FE model was validated through physical experiments.

The following conclusions with respect to the proposed sandwich configurations can be drawn:

- The internal angle, A , is an effective method of increasing the mechanical performance of the pyramidal structure.
- Among the studied configurations, C2 was proven to provide the best mechanical properties and represents be the best candidate for future investigations and optimizations.
- The pyramidal cellular structure under study shows a high potential in competing with other solutions based on different cellular topologies.

After completing the parametric study and the evaluation of the mechanical performances of the unit cell of the corrugation and of the associated sandwich panel, the following future research directions can be formulated:

- An optimization process can be conducted to increase of the mechanical properties of the pyramidal. The initial study could consider the angle A independent from the perforation radius R .
- The developed FE model could be furtherly improved to evaluate and compute the out-of-plane compression properties together with the analytical formulation.
- The overall bending performances may be increased by replacing the material of the core and face sheets with a high-end low-density material (e.g. aluminium, carbon fibre reinforced composites etc.). This will translate into a significant reduction in density for the associated sandwich assembly.

Personal and original contributions to the thesis

The investigation of the topology of novel pyramidal cellular core proposed for study was performed with the help of the parametric study conducted. The interdependence between the parameters of the unit cell has been defined and discussed, the formulations for computing the bulk dimensions of the core were presented.

The out-of-plane compressive properties were computed with the help of the analytical model developed. The formulation for determining the out-of-plane stiffness, E_z , and strength, σ_z were defined and validated through experimental procedures.

The bending and shear properties of the sandwich beam constructed with the novel pyramidal cellular core was evaluated by using the numerical and experimental approach. The setup for both virtual and physical experiments were developed and the correlation between the two was assessed and discussed.

The samples for the experimental models were created and tested accordingly to the conditions defined by the theoretical formulations.

Two comparative studies were conducted to evaluate the potential of the newly developed pyramidal core in comparison to the existing solutions in the literature. The structure obtained through a mechanical expansion process proved to be a promising alternative to be used as core in the construction of sandwich panels.

The results of the conducted research were disseminated in six scientific papers and articles. Four scientific papers were presented in international conferences, out of which three were published in their respective conference proceedings and one was included in the Scientific Bulletin of Transilvania University of Brasov.

Two articles were submitted to high impacted scientific journals from which one has already been published and the last is currently under review.

List of publications

1. **Ciolan (Iftimiciuc), M.A.**, Lache, S., Velea, M.N., *Cellular cores with negative Poisson's ratio for sandwich panels*, Bulletin of the Transilvania University of Brașov, Series I: Engineering Sciences, Vol. 10 (59) No. 2 – 2017. ISSN, Paper presented at the "3rd International Conference for Doctoral Students - IPC 2017", 22-23 June, Brașov, Romania.
2. **Iftimiciuc, M.A.**, Lache, S., Velea, M.N., *The auxetic behavior of an expanded periodic cellular structure*, AIP conference proceedings, vol. 1932, 030021 (2018), DOI: <https://doi.org/10.1063/1.5024171>, Online ISBN: 978-0-7354-1624-6 (indexed Web of Science). Paper presented at "The 7th International Conference on Structural Analysis of Advanced Materials", 19-22 September, Bucharest, Romania.

3. **Iftimiciuc, M.A.**, Lache, S., Velea, M.N., *Topologic Study of a Novel Periodic Cellular Core for Sandwich Panels*, IOP Conference Series: Materials Science and Engineering, Volume 416, 7th International Conference on Advanced Materials and Structures - AMS 2018, DOI: doi:10.1088/1757-899X/416/1/012087, (indexed Web of Science). Paper presented at "7th International Conference on Advanced Materials and Structures - AMS 2018", 28-31 March, Timisoara, Romania.
4. **Iftimiciuc, M.A.**, Velea, M.N., Lache, S., *In-plane transversal stiffness of expanded trapezoidal cellular structure*, The 8th International Conference on COMPUTATIONAL MECHANICS AND VIRTUAL ENGINEERING, 21-22 November, Brasov, Romania.
5. **Iftimiciuc, M.A.**, Lache, S., Wennhage, P., Velea, M.N., *Structural Performance Analysis of a Novel Pyramidal Cellular Core Obtained through a Mechanical Expansion Process*, Materials 2020, 13(19), 4264; <https://doi.org/10.3390/ma13194264>.
6. **Iftimiciuc, M.A.**, Lache, S., Vandepitte, D., Velea, M.N., *Bending performance of a sandwich beam with sheet metal pyramidal core* (under review).

References

1. Zenkert, D., *The handbook of sandwich construction*, Worcestershire: EMAS; 1997.
2. Velea, M.N., *Lightweight cellular Structures – Design, Modelling and Analysis*, Brasov: Editura Universitatii Transilvania din Brasov; 2011.
3. Clough, E.C., Ensberg, J., Eckel, Z.C., Ro, C.J., Schaedler, T.A., *Mechanical performance of hollow tetrahedral truss cores*, International Journal of Solids and Structures, 2016. 91: p. 115–126.
4. Vinson, J.R., Sandwich Structures: Past, Present, and Future. In: Thomsen O., Bozhevolnaya E., Lyckegaard A. (eds) *Sandwich Structures 7: Advancing with Sandwich Structures and Materials*, 2005. Springer, Dordrecht: p. 3-12.
5. Besse, C.C. and Mohr D., *Plasticity of formable all-metal sandwich sheets: Virtual experiments and constitutive modelling*, International Journal of Solids and Structures, 2012. 49: p. 2863-2880.
6. Garrido, M. and Correia, J.R., *Elastic and viscoelastic behaviour of sandwich panels with glass-fibre reinforced polymer faces and polyethylene terephthalate foam core*, Journal of Sandwich Structures and Materials, 2018. 20(4): p. 399–424.
7. Li, F.H., Han, B., Zhang, Q.C., Jin, F., Lu, T.J., *Buckling of a standing corrugated sandwich plate subjected to body force and terminal load*, Thin-Walled Structures, 2018. 127: p. 688–699.
8. Beharic, A., Rodriguez Egui, R., Yang, L., *Drop-weight impact characteristics of additively manufactured sandwich structures with different cellular designs*, Materials and Design, 2018. 145: p. 122-134.
9. Liu, T., Deng, Z.C., Lu, T.J., *Structural modelling of sandwich structures with lightweight cellular cores*, Acta Mechanica Sinica, 2007. 23: p. 545–559.
10. Bai, X., Zheng, Z., Nakayama, A., *Heat transfer performance analysis on lattice core sandwich panel structures*, International Journal of Heat and Mass Transfer, 2019. 143: p. 118525.
11. Regulation (EU) 2019/631 of the European Parliament and of the Council of 17th of April 2019 setting CO₂ emission performance standards for new passenger cars and for new light commercial vehicles and repealing Regulations (EC) No 443/2009 and (EU) No 510/2011.

12. Walsh, M. P., *Mobile Source Mitigation Opportunities. Chapter 6, Global Climate Change - The Technology Challenge*, New York, Springer, 2011.
13. Hou, S., Shu, C., Zhao, S., Liu, T., Xu Han, X., Li, Q., *Experimental and numerical studies on multi-layered corrugated sandwich panels under crushing loading*, Composite Structures, 2015. 126: p. 371–385.
14. Rejab, M.R.M., Ushijima, K., and Cantwell, W.J., *The shear response of lightweight corrugated core structures*, Journal of Composite Materials, 2014. 48(30): p. 3785–3798.
15. Ghabezi, P., *Rectangular and Triangular Corrugated Composite Skins*, Fibers and Polymers, 2018. 19(2): p. 435-445.
16. Keshavanarayana, S.R., Shahverdi, H., Kothare, A., Yang, C., Bingenheimer, J., *The effect of node bond adhesive fillet on uniaxial in-plane responses of hexagonal honeycomb core*, Composite Structures, 2017. 175: p. 111-122.
17. Ahmad, S., Zhang, J., Feng, P., Yu, D., Wu, Z., Ke, M., *Processing technologies for Nomex honeycomb composites (NHCs): A critical review*, Composite Structures, 2020. 250: p. 112545.
18. Wadley, H.N.G., Fleck, N.A, Evans, A.G., *Fabrication and structural performance of periodic cellular metal sandwich structures*, Composites Science and Technology, 2003. 63: p. 2331–2343.
19. Lia, D., Ma, J., Dong, L., Lakes, R.S., *Stiff square structure with a negative Poisson's ratio*, Materials Letters, 2017. 188: p. 149–151.
20. Huang, J., Zhang, Q., Scarpa, F., Liu, Y., Leng, J., *Bending and benchmark of zero Poisson's ratio cellular structures*, Composite Structures, 2016. 152: p. 729–736.
21. Lu, Z.X., Li, X., Yang, Z.Y., Xie, F., *Novel structure with negative Poisson's ratio and enhanced Young's modulus*, Composite Structures, 2016. 138: p. 243–252.
22. Xiong, J., Gu, D., Chen, H., Dai, D., Shi, Q., *Structural optimization of re-entrant negative Poisson's ratio structure, fabricated by selective laser melting*, Materials and Design, 2017. 120: p. 307–316.
23. Wang, Z.P., Poh, L.H., Zhu, Y., Dirrenberger, J., Forest, S., *Systematic design of tetra-petals auxetic structures with stiffness constraint*, Materials & Design, 2019. 170: p. 107669.
24. Wang H., Lu Z., Yang Z., Li X., *In-plane dynamic crushing behaviors of a novel auxetic honeycomb with two plateau stress*, International Journal of Mechanical Sciences, 2019. 151: p. 746-759.

25. Zhang, J., Lu, G., Ruan, D., Wang, Z., *Tensile behavior of an auxetic structure: Analytical modeling and finite element analysis*, International Journal of Mechanical Sciences, 2018. 136: p. 143-154.
26. Liu, C., Zhang, Y.X., and Heslehurst, R., *Impact resistance and bonding capability of sandwich panels with fibre-metal laminate skins and aluminium foam core*, Journal of Adhesion Science and Technology, 2014. 28:24: p. 2378-2392.
27. Hangai, Y., Kamada, H., Utsunomiya, T., Kitara, S., Kuwazuru, O., Yoshikawa, N., *Aluminum alloy foam core sandwich panels fabricated from die casting aluminum alloy by friction stir welding route*, Journal of Materials Processing Technology, 2014. 214: p.1928-1934.
28. Gonzalez Nava, M., Cruz-Ramírez, A., Suarez Rosales, M.A., Gutierrez-Perez, V.H., Sanchez-Martínez, A., *Fabrication of aluminum alloy foams by using alternative thickening agents via melt route*, Journal of Alloys and Compounds, 2017. 698: p. 1009-1017.
29. Wu, Q., Gao, Y., Wei, X., Mousanezha, D., Ma, L., Vaziri, A., Xiong, J., *Mechanical properties and failure mechanisms of sandwich panels with ultra-lightweight three-dimensional hierarchical lattice cores*, International Journal of Solids and Structures, 2018. 132–133: p. 171–187.
30. Sun, F., Lai, C., Fan, H., Fang, D., *Crushing mechanism of hierarchical lattice structure*, Mechanics of Materials, 2016. 97: p. 164–183.
31. Yin, S., Wu, L., Nutt, S., *Stretch–bend-hybrid hierarchical composite pyramidal lattice cores*, Composite Structures, 2013. 98: p. 153–159.
32. Wu Q., Vaziri, A., Eydani Asl, M., Ghosh, R., Ying, G., Wei X., Ma L., Jian, X., Wu L., *Lattice materials with pyramidal hierarchy: Systematic analysis and three dimensional failure mechanism maps*, Journal of the Mechanics and Physics of Solids, 2019. 125: p. 112-144.
33. Sorohan, S., Constantinescu, D.M., Sandu, M., Sandu, A.G., *In-plane homogenization of commercial hexagonal honeycombs considering the cell wall curvature and adhesive layer influence*, International Journal of Solids and Structures, 2019. 156–157: p. 87-106.
34. Nhi H.V., Thong M. P., Bi, K., Chen, W., Hao, H., *Stress Wave Mitigation Properties of Dual-meta Panels against Blast Loads*, International Journal of Impact Engineering, 2021. 154: p. 103877.
35. Wadley, H.N.G., *Multifunctional Periodic Cellular Metals*, Philosophical Transactions: Mathematical, Physical and Engineering Sciences, Engineered Foams and Porous Materials, 2006. 364(1838): p. 31-68.

36. Liu, Z., Lu, J., Zhu, P., *Lightweight design of automotive composite bumper system using modified particle swarm optimizer*, Composite Structures, 2016. 140: p. 630–643.
37. Eckstein, E., Pirrera, A., Weaver, P.M., *Multi-mode morphing using initially curved composite plates*, Composite Structures, 2014. 109: p. 240–245.
38. <http://www.nuplex.com/composites/processes/hand-lay-up>, 20.07.2017, 1.55 PM.
39. Ashori, A., *Wood-plastic composites as promising green composites for automotive industries*, Bioresource Technology, 2008. 99: p. 4664-4667.
40. Partanaen, A., Carus, M., *Wood and natural fiber composites current trend in consumer goods and automotive parts*, Reinforced plastics, 2016. 60(3).
41. Liu, Z., Lu, J., Zhu, P., *Lightweight design of automotive composite bumper system using modified particle swarm optimizer*, Composite Structures, 2016. 140: p. 630-643.
42. Li, H., Dai, F., Du, S., *Numerical and experimental study on morphing bi-stable composite laminates actuated by a heating method*, Composite science and technology, 2012. 72: p. 1767-1773.
43. Gibson, R.F., *A review of recent research on mechanics of multifunctional composite materials and structures*, Composite Structures, 2010. 92: p. 2793-2810.
44. Snudden, J.P., Ward, C., Potter, K., *Reusing automotive composites production waste*, Reinforced Plastics, 2014. November/December: p. 20-27.
45. Sayahlatifi, S., Rahimi, G. and Bokaei, A., *Experimental and numerical investigation of sandwich structures with balsa core and hybrid corrugated composite/balsa core under three-point bending using digital image correlation*, Journal of Sandwich Structures & Materials, 2021. 23(1): p. 94–131.
46. Faris M.A., Sapuan, S.M., *Natural fiber reinforced polymer composites in industrial applications: feasibility of date palm fibers for sustainable automotive industry*, Journal of Cleaner Production, 2014. 66: p.347-354.
47. Sobczak, L., Lang, R.W., Haider, A., *Polypropylene composites with natural fibers and wood – General mechanical property profiles*, Composites Science and Technology, 2012. 72(5):p. 550-557.

48. Sailesh, A., Arunkumar, R., Saravanan, S., *Mechanical Properties and Wear Properties of Kenaf – Aloe Vera – Jute Fiber Reinforced Natural Fiber Composites*, Materials Today: Proceedings, 2018. 5(2): p. 7184-7190.
49. Monteiro, S.N., Calado, V., Rodriguez, R.J.S., Margem, F.M., *Thermogravimetric behavior of natural fibers reinforced polymer composites - An overview*, Materials Science and Engineering: A, 2012. 557: p. 17-28.
50. Alves, C., Ferraõ, P.M.C., A.J., Silva, A.J., L.G. Reis, L.G., Freitas, M., Rodrigues, L.B., Alves, D.E., *Ecodesign of automotive components making use of natural jute fiber composites*, Journal of Cleaner Production, 2010. 18: p. 313–327.
51. Velea, M.N., Lache, S., *In-plane effective elastic properties of a novel cellular core for sandwich structures*, Mechanics of Materials, 2011. 43(7): p.377-388.
52. Czarnecki, T., Sewell, J., Pflug, J., *EconCore developing high performance thermoplastic honeycomb core materials*, Reinforced Plastics, 2019. 63(3).
53. Li, T., Wang, L., *Bending behavior of sandwich composite structures with tunable 3D-printed core materials*, Composite Structures, 2017. 175: p. 46–57.
54. Tubío, C.R., Gutián, F., Alvaro G., *Fabrication of ZnO periodic structures by 3D printing*, Journal of the European Ceramic Society, 2016. 36: p. 3409–3415.
55. Vogiatzis, P., Chen, S., Wang, S., Li, T., Wang, L., *Topology optimization of multi-material negative Poisson's ratio metamaterials using a reconciled level set method*, Computer-Aided Design, 2017. 83: p. 15-32.
56. Kang, K.J., *Wire-woven cellular metals: The present and future*, Progress in Materials Science, 2015. 69: p. 213–307.
57. Lee, M.G., Yoon, J.W., Han, S.M., Suh, Y.S., Kang, K.J., *Bending response of sandwich panels with discontinuous wire-woven metal cores*, Materials and Design, 2014. 55: p. 707-717.
58. Zhou, X., Wang, H., You, Z., *Mechanical properties of Miura-based folded cores under quasi-static loads*, Thin-Walled Structures, 2014. 82: p. 296–310.
59. Pydah, A., Batra, R.C., *Crush dynamics and transient deformations of elastic-plastic Miura-ori core sandwich plates*, Thin-Walled Structures, 2017. 115: p. 311-322.

60. Velea, M.N., Schneider, C., Lache, S., *Second order hierarchical sandwich structure made of self-reinforced polymers by means of a continuous folding process*, Materials and Design, 2016. 102: p. 313–320.
61. Khan, M.S., S.S.R., and Tamin, M.N., *Effects of cell aspect ratio and relative density on deformation response and failure of honeycomb core structure*, Materials Research Express, 220. 7: p. 015332
62. Crupi, V., Epasto, G., Guglielmino, E., *Comparison of aluminium sandwiches for lightweight ship structures: Honeycomb vs. foam*, Marine Structures, 2013. 30: p. 74–96.
63. Tao, Y., Chen, M., Chen, H., Pei, Y., Fang, D., *Strain rate effect on the out-of-plane dynamic compressive behavior of metallic honeycombs: Experiment and theory*, Composite Structures, 2015. 132: p. 644–651.
64. Wu, Y., Liu, Q., Fu, J., Li, Q., Hui, D., *Dynamic crash responses of bio-inspired aluminum honeycomb sandwich structures with CFRP panels*, Composites Part B, 2017. 121: p. 122–133.
65. Thomas, T. and Tiwari, G., *Crushing behavior of honeycomb structure: a review*, International Journal of Crashworthiness, 2019 (24): p. 555–579.
66. Bitzer, T.N., *Honeycomb Technology*, Materials, Design, Manufacturing, Applications and Testing. 1997: Springer Science + Business Media, B.V.
67. Wadley, H.N.G., Fleck, N.A. and Evans, A.G., *Fabrication and Structural Performance of Periodic Cellular Metal Sandwich Structure*. Composites Science and Technology, 2003. 63: p. 2331–2343.
68. Shafizadeh, J.E., *Evaluation of the in-service performance behavior of honeycomb composite sandwich structures*. Journal of Materials Engineering and Performance, 1999. 8(6): p. 661–668.
69. Wang, Y.J., Zhang, Z.J., Xue, X.M., Zhang, L., *Free vibration analysis of composite sandwich panels with hierarchical honeycomb sandwich core*, Thin-Walled Structures, 2019. 145: p. 106425.
70. Hou, X., Deng, Z., Zhang, K., *Dynamic Crushing Strength Analysis of Auxetic Honeycombs*, Acta Mechanica Solida Sinica, 2016. 29(5).
71. Queheillalt, D.T., Wadley, H.N.G., *Titanium alloy lattice truss structures*, Materials and Design, 2009. 30: p. 1966–1975.
72. Sypek, D.J., *Cellular Truss Core Sandwich Structures*, Applied Composite Materials, 2005. 12: p. 229–246.

73. Iftimiciuc, M.A., Lache, S., Wenhage, P., Velea, M.N., *Structural Performance Analysis of a Novel Pyramidal Cellular Core Obtained through a Mechanical Expansion Process*, Materials, 2020. 13 (19): p. 42-64.
74. Iftimiciuc, M.A., Lache, S., Vandepitte, D., Velea, M.N., *Bending performance of a sandwich beam with sheet metal pyramidal core*, (under review).
75. Biagi, R., Bart-Smith, H., *In-plane column response of metallic corrugated core sandwich panels*, International Journal of Solids and Structures, 2012. 49(26): p. 3901-3914.
76. Velea, M.N., Lache, S., *Numerical simulations of the mechanical behavior of various periodic cellular cores for sandwich panels*, Procedia Engineering, 2011. 10: p. 287–292.
77. He, W., Liu, J., Tao, B., Xie, D., Liu, J., Zhang, M., *Experimental and numerical research on the low velocity impact behavior of hybrid corrugated core sandwich structures*, Composite Structures, 2016. 158(15): p. 30-43.
78. Velea, M.N., Wenhage, P., Lache, S., *Out-of-plane effective shear elastic properties of a novel cellular core for sandwich structures*, Materials & Design, 2012. 36(1980-2015): p. 679-686.
79. Iftimiciuc, M.A., Lache, S., Velea, M.N., *Topologic Study of a Novel Periodic Cellular Core for Sandwich Panels*, IOP conference series. Materials Science and Engineering, 2018. 416(1): p. 12087.
80. Castigliano, C.A., *Intorno ai sistemi elastici*. 1873, Politecnico di Torino: Torino.
81. Bartolozzi, G., Pierini, M., Ulf, O., Baldanzini, N., *An equivalent material formulation for sinusoidal corrugated cores of structural sandwich panels*. Composite Structures, 2013. 100(0): p. 173-185.
82. Bartolozzi, G., Baldanzini, N. and Pierini, M., *Equivalent properties for corrugated cores of sandwich structures: A general analytical method*. Composite Structures, 2014. 108: p. 736-746.
83. Shaban, M., Alibegloo, A., *Three-dimensional elasticity solution for sandwich panels with corrugated cores by using energy method*, Thin-Walled Structures, 2017. 119: p. 404-411.
84. Shu, C., Hou, S., *Theoretical prediction on corrugated sandwich panels under bending loads*, Acta Mechanica Sinica, 2018. 34(5): p. 925–935.
85. Qiao, P., Davalos, J.F., *Developments in Fiber-Reinforced Polymer (FRP) Composites for Civil Engineering*, Woodhead Publishing Series in Civil and Structural Engineering, 2013. Chapter 17 - *Design of all composite structures using fiber-reinforced polymer (FRP) composites*, p. 469-508.

86. Ju C., Young, B., *Stress-strain curves for stainless steel at elevated temperatures*, Engineering Structures, 2006. 28: p. 229–239.
87. Xiong, J., Ma, L., Vaziri, A., Yang, J., Wu, L., *Mechanical behavior of carbon fiber composite lattice core sandwich panels fabricated by laser cutting*. Acta Materialia, 2012. 60(13–14): p. 5322–5334.
88. Queheillalt, D.T. and Wadley, H.N.G., *Cellular metal lattices with hollow trusses*, Acta Materialia, 2005. 53(2): p. 303-313.
89. Li, M., Wu, L., Ma, L., Wang, B., Guan, Z., *Mechanical Response of All-composite Pyramidal Lattice Truss Core Sandwich Structures*, Journal of Materials Science & Technology, 2011. 27(6): p. 570–576.
90. Xiong, J., Ma, L., Wu, L., Wang, B., Vaziri, A., *Fabrication and crushing behavior of low density carbon fiber composite pyramidal truss structures*. Composite Structures, 2010. 92(11): p. 2695–2702.
91. ABAQUS, 2017. *Geometric imperfections, Abaqus analysis user's manual*. Dassault Systèmes.
92. Zhang, F., Liu, W., Fang, H., Jia, Z., *Flexural behavior of composite sandwich beams with different kinds of GFRP ribs in flatwise and edgewise positions*, Composites Part B 2019. 156: p. 229–239.